https://doi.org/10.5194/essd-2026-109
Preprint. Discussion started: 13 May 2026

Open Access Earth System Science Data Discussions

A Comprehensive Global Aquatic N_2O Emission Database (GANED): Unravelling N_2O Emission Patterns from Different Water Bodies

Muhammad Junaid Nazir[1, #], Longfei Yu[1, #], Yunjie Zhang[2], Jing Zou[2], Wenping Yuan[3], Jing Wei[2, *]

[1]Shenzhen Key Laboratory of Ecological Remediation and Carbon Sequestration, Institute of Environment and Ecology, Tsinghua Shenzhen International Graduate School, Tsinghua University, Shenzhen 518055, China.
[2]School of Atmospheric Sciences, Guangdong Province Data Centre of Terrestrial and Marine Ecosystems Carbon Cycle, Sun Yat-sen University, Zhuhai, Guangdong, 519082, China.
[3]Institute of Carbon Neutrality, Sino-French Institute for Earth System Science, College of Urban and Environmental Sciences, Peking University, Beijing, 100871, China.

Correspondence to: * Jing Wei (sarawei.em@gmail.com); # These authors contributed equally to this study.

Abstract. Nitrous oxide (N_2O) is not only one of the main potent greenhouse gases, but also currently the dominant ozone-depleting substance. The quantification of N_2O emissions from aquatic ecosystems, despite their global importance, is hindered by fragmented observations, inconsistent data reporting, and pronounced spatiotemporal variability. In this study, to improve accessibility, we introduce the Global Aquatic N_2O Emission Database (GANED; https://doi.org/10.6073/pasta/4a086e49a4f308679b951293b380e7b9, Nazir et al., 2026), a consolidated dataset comprising 5130 N_2O concentration records and 7386 N_2O flux measurements from 3002 sites across diverse aquatic systems including rivers, streams, lakes, reservoirs, ponds, estuaries, coastal waters, and open seas. The dataset integrates information on aquatic N_2O emission from 426 peer-reviewed publications across 8 continents, covering the period 1980-2023. While the number of observations has increased substantially since 2000, spatial coverage remains uneven, with significant gaps across Africa and parts of high-latitude regions, including Antarctica and South America. Our dataset revealed a highly skewed distribution of N_2O concentration and flux across aquatic ecosystems, with rivers and streams exhibiting the most significant variability and functioning as emission hotspots. Lakes and estuaries showed moderate variability and emission levels, whereas seas and coastal waters were characterized by consistently lower values. Pearson correlation coefficient revealed a strong positive relationship of N_2O fluxes with ammonium (NH_4^+; $R = 0.943$, $p < 0.001$), nitrate (NO_3^-; $R = 0.691$, $p < 0.001$), and nitrite (NO_2^-; $R = 0.807$, $p < 0.001$). Significant negative correlations were found with dissolved oxygen (DO; $R = -0.205$, $p < 0.05$), dissolved organic carbon (DOC; $R = -0.977$, $p < 0.05$), and salinity ($R = -0.636$, $p = 0.005$), while non-significant associations were observed for water temperature, total nitrogen (TN), and total phosphorus (TP). The GANED dataset facilitates improved quantification of global aquatic N_2O inventories by providing comprehensive N_2O concentrations and fluxes in water bodies, as well as metadata describing sampling location, aquatic system type, and associated environmental parameters. The magnitude and patterns of N_2O emissions from water bodies provided by the GANED database are essential in defining how these aquatic ecosystems shape our climate, refining emission estimates, identifying drivers, and guiding mitigation strategies.

https://doi.org/10.5194/essd-2026-109
Preprint. Discussion started: 13 May 2026

Open Access Earth System Science Data Discussions

1 Introduction

Nitrogen (N) processes in terrestrial and aquatic ecosystems are primary source of atmospheric nitrous oxide (N_2O), a potent long-lived greenhouse gas (GHG) with a global warming potential 273 times higher than that of carbon dioxide (CO_2), and the leading anthropogenic driver of stratospheric ozone depletion (Marzadri et al., 2021; Tian et al., 2024; Ravishankara et al., 2009; Masson-Delmotte, 2024). Human activities, particularly agricultural intensification through large-scale synthetic fertilizer production via the Haber-Bosch process, have significantly perturbed the global N cycle. As a result, the atmospheric N_2O concentration has increased by ~25% above pre-industrial levels, with a current growth rate of 1.05 ppb yr^{-1} (IPCC, 2023; Water, 2019). Over the past four decades, global N_2O emissions have significantly increased by over 24%, rising from 270 ppb to 336 ppb (Christensen and Rousk, 2024), consequently contributing to 6.4% of total GHG radiative forcing over the period of 1750-2022 (IPCC, 2022; Gong et al., 2024). Recent estimates reveal consistent upward trends in global N_2O emissions, with both bottom-up assessments reporting an increase from 17.4 Tg N yr^{-1} to 18.5 Tg N yr^{-1}, corresponding to an average increase rate of 0.043 Tg N yr^{-2} (Yao et al., 2020), and top-down estimates indicating an increase from 15.4 Tg N yr^{-1} to 17.0 Tg N yr^{-1} over the period 1997-2020, reflecting a higher average rate of 0.085 Tg N yr^{-2} (Tian et al., 2024). These divergent rates are primarily attributed to the continuous increase in N_2O emissions from both terrestrial and aquatic sources owing to increased food, feed, and energy demands (Davidson and Kanter, 2014).

Aquatic ecosystems contributed approximately 25-32% (5.3 Tg N yr^{-1}) of the total global N_2O emissions in 2020, second only to soils (Tian et al., 2020; Zheng et al., 2022; Zhang et al., 2024). These aquatic ecosystems, including inland waters (rivers, reservoirs, lakes, ponds, streams), estuaries, coastal zones, and oceans, represent significant yet highly uncertain sources of atmospheric N_2O (Wang et al., 2021a; Duvert et al., 2025). Inland waters emitted ~319.6 ± 58.2 Gg N yr^{-1} of N_2O during the 2010s, representing an increase of about 207 Gg N yr^{-1} since the 1850s, with riverine systems contributing ~80% and lakes and reservoirs ~20% (Li et al., 2024). Consequently, N inputs from both agricultural and non-agricultural sources have made rivers, lakes, and reservoirs substantial contributors to the global N_2O budget (Zheng et al., 2022; Tian et al., 2024). Global riverine emissions are estimated at 30-35 Gg N_2O-N yr^{-1}, representing 0.16-0.19% of dissolved inorganic nitrogen (DIN) entering streams (Hu et al., 2016). Similarly, Zhang et al. (2026) reported that aquatic N_2O emissions are highest in the downstream reaches of reservoirs and in regions with dense populations and intensive agricultural activity, notably in eastern and southern Asia, southeastern North America, and Europe.

In aquatic ecosystems, N_2O production arises from complex microbial (nitrification, denitrification) and abiotic (chemodenitrification) pathways, modulated by nutrient supply, dissolved oxygen, water temperature, N, phosphorus (P), and pH (Tian et al., 2020; Wei et al., 2022; Pan et al., 2023). Aquatic N_2O emissions regulated by these key drivers vary widely by aquatic system types. Rivers exhibit increased fluxes driven by rapid water turnover and anthropogenic N loading, exacerbating eutrophication, warming, and pollution (Lu et al., 2023). Reservoirs and lakes are governed by stratification, with hypolimnetic anoxia favoring denitrification, triggering pulse N_2O releases (He et al., 2023). Similarly, estuaries function as hotspots, where high nutrient and organic matter inputs, coupled with hydrodynamic mixing, stimulate coupled nitrification and denitrification (e.g., Yangtze River estuary; Liu et al., 2025). Further, streams and ponds, despite their small size, have also been identified as

https://doi.org/10.5194/essd-2026-109
Preprint. Discussion started: 13 May 2026

important sources of N_2O to the atmosphere due to high per-area fluxes from intense microbial activity and recurrent anoxia (Saunois et al., 2020; Bodmer et al., 2021). Oceans and coastal seas remain the largest contributors to global aquatic N_2O emissions, with oxygen-deficient zones disproportionately responsible for more than half of the total flux (Wang et al., 2025; Rees et al., 2022). Besides being predominantly sources of N_2O, some aquatic systems exhibit modest sink potentials. In undersaturated oceanic regions, atmospheric N_2O is absorbed and microbially consumed, sequestering 0.1-0.3 Tg N yr^{-1} (De La Paz et al., 2025; Tian et al., 2024). Inland waters may also exhibit temporary sink function under precipitation-driven anoxia, reducing N_2O to N_2 (Liang et al., 2023). Although the net sink contribution of aquatic systems is minor compared with emissions, the sink processes of N_2O prior to emission could be important for unraveling spatiotemporal variabilities as well as for regional-global predictions (Zhang et al., 2024), considering the large potential for gross N_2O production in generally anaerobic aquatic environments (Wang et al., 2025).

Despite the importance of constraining N_2O budgets from aquatic ecosystems, substantial uncertainties persist due to a combination of spatial heterogeneity, data gaps, limited temporal coverage, environmental variability, and methodological inconsistencies. Higher emissions in regions with intensive anthropogenic activities, such as eastern and southern Asia, the southeastern United States, and parts of Europe, lead to significant spatial heterogeneity (Song et al., 2024; Wang et al., 2023). Tropical, arid, and high-latitude regions are poorly explored, limiting accurate upscaling to the global budget. Temporal variabilities, driven by rapid water turnover, or temporal events including eutrophication, warming, pollution, and precipitation-driven anoxia, are likely to contribute to pulse N_2O releases which are hard to measure (Zheng et al., 2022). Furthermore, production and emission processes are strongly influenced by local environmental factors, such as nutrient loading from fertilizers and manure, organic matter decomposition, agricultural runoff, salinity, and urbanization, leading to significant spatiotemporal variability (IPCC, 2023; Resplandy et al., 2024). Additionally, methodological differences introduce another major source of uncertainty, as different flux estimates frequently arise from the use of diverse measurement techniques. For example, variation in gas-transfer velocity (k) parameterizations and differences between chamber-based and concentration-gradient approaches can lead to flux discrepancies of 30-70%, depending on the methods and underlying assumptions (Hall Jr and Ulseth, 2020; Stanley et al., 2022). These differences highlight the difficulty of comparing flux data among aquatic types. For instance, fluxes are often much higher in some high-emission environments (e.g., estuaries) than in lower-emitting systems such as lakes and reservoirs. Collectively, these inconsistencies restrict the further consolidation of the global aquatic N_2O emission inventories, highlighting the need for improved monitoring networks, standardized methods, and better coverage of underrepresented areas to reduce uncertainties and refine global N_2O budgets.

The main objectives of this study are to: (1) construct a harmonized database for data acquisition and observation; (2) characterize the distributional patterns of N_2O concentrations and fluxes across various aquatic ecosystems; and (3) identify existing data gaps and propose future research directions to advance the understanding of N_2O dynamics in aquatic ecosystems. To achieve these objectives and to evaluate and predict N_2O emissions from aquatic ecosystems accurately, we developed a comprehensive database, the Global Aquatic N_2O Emission Database (GANED). This database compiles records from 3002 sites to investigate global distributional patterns of both N_2O concentrations and fluxes across aquatic ecosystems, linked with

https://doi.org/10.5194/essd-2026-109
Preprint. Discussion started: 13 May 2026

associated biogeochemical variables. It also addresses discrepancies between concentration and flux observations, enabling robust cross-system comparisons and improved prediction of aquatic N_2O emissions. By describing the dataset structure and outline, we demonstrated its potential to reveal spatial, temporal, and biogeochemical controls on N_2O dynamics across diverse aquatic systems. By integrating these attributes, GANED provides: (i) in-depth analyses of N_2O drivers, seasonal and spatial variability; (ii) upscaling supports to improving national GHG inventories and global modeling frameworks; and (iii) robust empirical evidence and theoretical basis for the quantitative assessment and management of aquatic N_2O emissions.

2 Methods

2.1 Literature search and data extraction

We conducted a comprehensive and systematic literature review of studies published in peer-reviewed journals between 1980 to 2023, following guidelines consistent with the Preferred Reporting Items for Systematic Reviews and Meta-Analyses (PRISMA) framework, adapted for database synthesis (Moher et al., 2014). To synthesize GANED, original experimental data were extracted directly from publications reporting N_2O concentrations and fluxes from aquatic systems, including rivers, reservoirs, lakes, ponds, streams, estuaries, coastal areas, and seas (Fig. 1). GANED consolidates four interlinked datasets encompassing (1) data sources, (2) sampling sites, (3) N_2O concentrations, and (4) N_2O fluxes, accompanied by associated physicochemical parameters such as ammonium (NH_4^+), nitrate (NO_3^-), nitrite (NO_2^-), dissolved oxygen (DO), dissolved organic carbon (DOC), total nitrogen (TN), total phosphorus (TP), water temperature, salinity and pH, along with supporting metadata such as geographic location, sampling dates, temporal information, climate data, and methodological details. These datasets were connected through unique source identifiers, with each concentration and flux record assigned a distinct site number to ensure consistency and traceability across data tables. Arrow lines illustrate the data flow and relational structure among these datasets. Data compiled in GANED were sourced from peer-reviewed journal articles, master's theses, and doctoral dissertations that reported quantitative N_2O measurements. Source material was obtained through systematic searches of major bibliographic databases and repositories, including Web of Science, Scopus, and Google Scholar, using combinations of the keywords including "nitrous oxide/N_2O", "river", "stream", "reservoir," "lake", "pond", "estuary", "coastal", "sea", and "ocean" as depicted in Fig. 1.

Inclusion criteria were rigorously applied to data reliability across studies. Specifically, (1) sources must report direct measurements of N_2O concentrations or fluxes from aquatic ecosystems; (2) datasets must include geospatial coordinates or clearly identifiable sampling site locations; (3) peer-reviewed journal articles, and dissertations/theses were prioritized, though selected reports were incorporated if they provided novel data; (4) measurements must be accompanied by key environmental variables, e.g., NH_4^+, NO_3^-, NO_2^-, DO, DOC, TN, TP, water temperature, salinity and pH, to facilitate analysis of N_2O drivers. Exclusion criteria were applied to eliminate studies that focused exclusively on terrestrial soils, atmospheric modeling without empirical validation, or those lacking quantitative data, such as qualitative reviews. Following this screening process, a total of 426 data sources met the inclusion requirements, comprising approximately 400 peer-reviewed journal articles and 26

https://doi.org/10.5194/essd-2026-109
Preprint. Discussion started: 13 May 2026

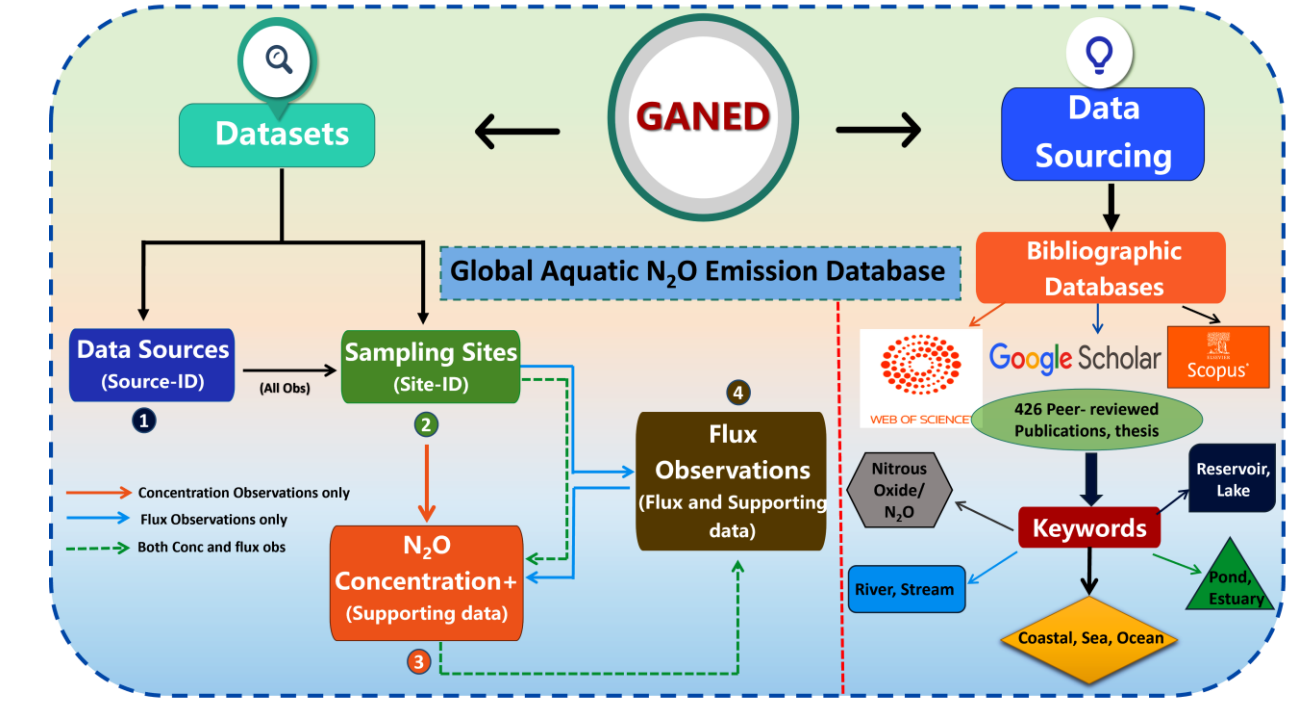

Figure 1: Schematic overview of GANED and the relationship among its four meta-datasets. The data workflow began with recording metadata for each source in the "Data Source", where a unique 'Source-ID' was assigned. Site-specific information from each source was then entered into the "Sampling Sites", with each site allocated a unique 'Site-ID' that was cross-referenced with its corresponding Source-ID. Both identifiers (Source-ID and Site-ID) were subsequently carried into the "Concentration and Flux" datasets to ensure complete traceability across all observations. N_2O observations were categorized based on site-date combinations, distinguishing between concentration data (orange) and flux data (blue) arrow lines. The "Concentration & Flux" datasets recorded Concentration records and flux measurements along with supporting data, respectively. Data sourcing for GANED carried through deep searching of the bibliographic databases (Web of Science, Google Scholar, Scopus) and related keywords.

2.2 Database Structure

The structure of GANED built upon established frameworks from analogous compilations in aquatic GHG research. Adapting this research approach, GANED was structured into four interrelated components, each designed to facilitate seamless data integration and analytical flexibility. These components were interconnected via unique identifiers for both data sources and sampling sites, allowing users to trace each observation to its origins while exploring spatiotemporal patterns and environmental correlates. The "Data Source" dataset stored metadata of each publication or report, uniquely identified by a 'Source-ID'. The "Sampling Sites" dataset recorded information for each observational site, each associated with its corresponding data source through the same 'Source-ID'. These identifiers were used to associate site-level attributes with the "N_2O Concentration" and "N_2O Flux" datasets, ensuring consistent referencing and integrity. This structured linkage enabled robust integration, filtering, and querying across datasets, thereby supporting advanced analyses of spatial and temporal N_2O

https://doi.org/10.5194/essd-2026-109
Preprint. Discussion started: 13 May 2026

variability. The database also included flags for data aggregation (spatial and temporal) and observation types, allowing users to filter the dataset for methodological consistency. Thus, this modular design not only aligned with successful precedents in aquatic GHG databases but also enhanced usability for hypothesis testing and upscaling exercises specific to N_2O dynamics. The data workflow for N_2O observations is further demonstrated in Fig. 2.

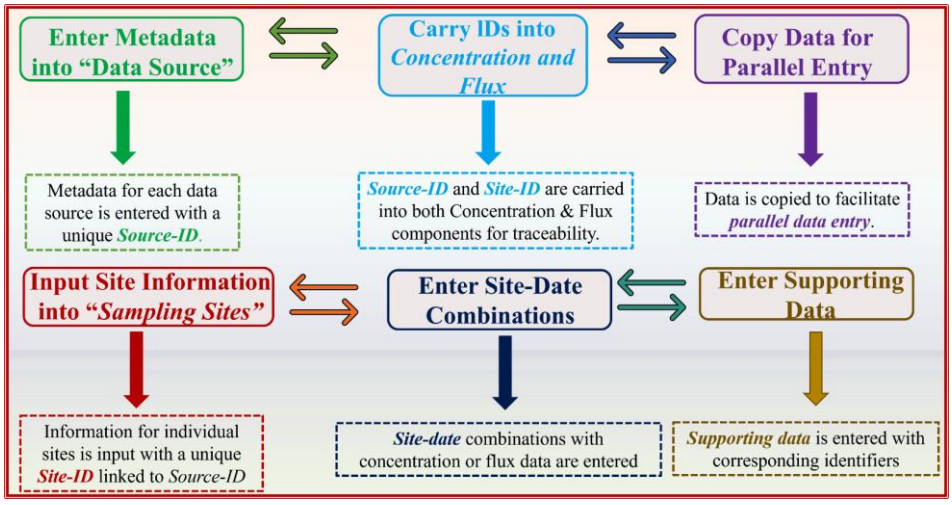

Figure 2: Workflow for entering data into the GANED. A structured, step-by-step protocol for inputting metadata, site-specific information, and ancillary concentration and flux datasets into the system, ensuring rigorous data integrity and streamlined processing through standardized workflows.

2.2.1 Data Source

The "Data Source" component comprised of all scientific literature used in constructing GANED. Each N_2O data source was identified by a unique 'Source-ID' along with corresponding bibliographic details, including title (Title), author(s) (Author), publication type (Type), data source name (SRC-Name), publication year (Pub-year), and digital object identifiers (DOI). All column titles for "Data Source" are provided in Table A1. In several instances, the compiled datasets were supplemented with additional information, including related physicochemical parameters sourced from external databases or obtained directly from the original author(s) to clarify incomplete or ambiguous records. To resolve uncertainties (e.g., unit inconsistencies) or to acquire missing/more detailed information (e.g., site- or date-specific concentrations or fluxes), we contacted the corresponding authors as well to verify or provide supplementary data. The source dataset represented the integration of previously unpublished data provided by these authors, along with a detailed account of all modifications and corrections.

2.2.2 Sampling Sites

Site-specific information was extracted from tables, figures, and text descriptions provided by the authors within the source publications using Web-Plot-Digitizer (https://automeris.io/WebPlotDigitizer/). This process yielded geospatial and descriptive attributes for the 3002 unique sampling sites, including information on country, continent, aquatic type, site name, channel

https://doi.org/10.5194/essd-2026-109
Preprint. Discussion started: 13 May 2026

type, latitude, longitude, depth (m), surface area (km^2), elevation (m), and status (e.g., concentration-only, flux-only, or both). The "Sampling Sites" dataset summarized the basic attributes of all locations where N_2O measurements were collected. Each site is assigned a unique identifier 'Site-ID' and a corresponding site name (typically taken directly from the original data source/publication). Sites were also cross-referenced with the "Data Source" dataset through the shared 'Source-ID'. A detailed description of all columns included in the "Sampling Site" dataset is provided in (Table A2).

The spatial extent associated with each 'Site-ID' varied among data sources. In some cases, sites represented (1) discrete sampling points, (2) geomorphically distinct study reaches, or (3) large channel sections, drainage networks, or other defined geographic units. For sites containing multiple sampling points, results were generally averaged to represent mean conditions. Most of the sites had geographic coordinates, though in cases where coordinates were missing, approximate locations were derived from maps or figures in the original publications using Google Earth (Google, 2025, https://earth.google.com/). All coordinates were verified and corrected as needed to minimize spatial errors. Gas sampling at closely located sites (often referred to as 'high-density sites') can complicate site delineation and data interpretation. To address this, we merged data from points with minimal differences in latitude and longitude, treating them as a single representative site. For that, firstly, latitude and longitude precision were standardized to three decimal places to ensure spatial consistency. Secondly, in cases where samples were collected from multiple points or depths within a single channel cross-section, data were averaged to produce one representative record (especially for the Pearl River basin and the streams in Guangdong Province, China). However, some ambiguity remained when distinguishing between repeated observations at the same site and distinct nearby locations (typically 10-50 m apart). In such instances, sites with overlapping coordinates and sampling on different days were treated as a single site based on careful evaluation.

Many studies on aquatic N_2O dynamics aimed to determine whether, and to what extent, specific features such as upstream reservoirs, point-source discharges, thermokarst formations, or gas extraction activities affect N_2O concentrations and fluxes, typically with the presumption of an overall acceleration. Similarly, investigations focusing on N_2O hotspots (e.g., springs, floodplains, backwaters, ditches, or canals) might introduce a bias toward higher emission estimates (Stanley et al., 2022). Nevertheless, we still included these data points in GANED, allowing us to examine the outcomes of anthropogenic influence on aquatic N_2O emission. Additionally, to enhance interpretability, we devised a system of channel codes to be used when identifying intended site types. The description of channel codes has been demonstrated in Table 1. Standardizing these classifications posed significant challenges, often requiring subjective judgment in the context of N_2O emissions from aquatic systems. For example: (1), the influence of upstream dam (code US) on downstream sites (code DS) varied with distance (Wang et al., 2021b); (2) symmetric linear canals in agricultural and urban areas had unclear origins, with uncertainty over whether natural streams were channelized (code CH) or new ditches/canals (codes DIT, CAN) were created; in this case unspecified straight channels were coded as CH (3) wetland springs (WTS) were frequently difficult to locate due to their diffuse boundaries; and (4) floodplain channels (FP) posed complexities in distinguishing riverine from wetland systems; therefor, the FP code was applied to lentic habitats such as backwaters or connected floodplain lakes. Due to these ambiguities, we recommend that these channel-type codes be interpreted with caution in conducting comparative or spatial analyses of

https://doi.org/10.5194/essd-2026-109
Preprint. Discussion started: 13 May 2026

aquatic N_2O emissions.

Table 1: Codes indicating site- or channel-specific attributes, as well as the presence of conditions potentially influencing N_2O concentrations or fluxes. Imposition of codes was based on information provided in the data source and/or direct observation of the site. Codes are recorded in the Channel-type field of the component "Sampling Sites" dataset.

Code	Description
CAN	A canal or artificial channel having hardened channel boundaries.
CH	Channelized (A channel, in which all or most of its straight-line segments are of the same width and variations of channel direction are usually angled features instead of curves).
CD	Channel in a river delta
US	Upstream: direction of water toward the source or origin of a river or stream.
DS	Downstream: Site or region farther away from the source, usually at a lower elevation.
DIT	Ditch, normally agricultural drainage, an unhardened channel
FP	Flood plain site in a water body linked to the main channel that is lentic or is defined as a floodplain lake or a backwater.
GT	The end or "toe' of a glacier, where the glacier's forward movement (advancing) or melting (retreating) stops.
IMP	The existence of more than one and typically small impoundment in the vicinity of a site (e.g., several rivers in Europe).
PI	permafrost that influences the local environment, particularly in regions adjacent to thermokarst outflows.
PSD	At once (< 1 km) downstream of any point source discharge.
SP	A spring channel is a natural or artificial pathway that directs water from a spring to other areas, such as rivers, streams, or reservoirs.
TH	The location that naturally receives thermogenic N_2O or by anthropogenic activities.
WTS	Wetland stream; the location is in a wetland or directly downstream of the outlet of a wetland.

2.2.3 Concentration and flux dataset

GANED was integrated with two core datasets, "N_2O Concentration" and "N_2O Flux", extracted from diverse global aquatic systems across various temporal and spatial scales. Both datasets were linked to the "Data Sources" and "Sampling Sites" via 'Source-ID' and 'Site-ID'. The datasets were further structured to include associated GHG measurements (CO_2, CH_4), as well as physical and chemical parameters to facilitate comprehensive analysis of N_2O dynamics (see Tables A3 and A4 for a complete list of columns and their descriptions). Most concentration and flux data were directly extracted from the tables of peer-reviewed literature, unpublished field measurements, and existing repositories provided by the authors. In some instances,

https://doi.org/10.5194/essd-2026-109
Preprint. Discussion started: 13 May 2026

values were obtained from figures, and data were digitized and standardized to ensure consistency within the database. Temporal precision varied across sites; some records specified exact days and months, while others reported only the month or year. To standardize the temporal resolution, all data were adjusted to a monthly level. For records lacking specific start dates, two additional columns "Sampling-Year" and "Sampling-Month" were introduced to indicate the month and year of data collection. Temporal aggregations were recorded in the "Aggregated-Time" field, which was marked as "No" when the start date (Date-start) and end dates (Date-end) were identical. Spatially aggregated sampling points were indicated by the "Aggregated-Space" field and marked as "Yes" when the mean value of the aggregated points was used to represent the data.

Measuring both dissolved N_2O concentration and flux from aquatic systems involved a combination of sampling techniques, gas analyses, and, in some cases, mathematical modeling. Among the recorded data sources, 52% of the total observations used a common approach of combined measurements of dissolved gas concentration (conc) and the gas exchange coefficient (k) to estimate N_2O emissions. Direct gas sampling followed by analysis via gas chromatography or mass spectrometry was also commonly employed. Additionally, chamber-based flux measurements, comprising 48% of all observations, were also widely used, such as floating and static chambers. In the chamber method, the flux rate was calculated based on the change in N_2O concentration within the chamber over time according to the Eq. (1):

$$FN_2O = \frac{V_{\text{chamber}} \cdot \Delta CN_2O}{A_{\text{surface}} \cdot \Delta t} \quad (1)$$

Where FN_2O is the N_2O flux ($\mu mol^{-2}day^{-1}$), $V_{chamber}$ is the chamber volume (L), ΔCN_2O is the observed change in N_2O concentration inside the chamber ($\mu molL^{-1}$), $A_{surface}$ is the chamber surface area (m^2), and Δt is the duration of the chamber deployment (in days).

N_2O flux via gas transfer velocity was typically calculated using the Eq. (2) (Henry's Law Method):

$$Flux = k \times \Delta C / H \quad (2)$$

Where Flux represents N_2O flux, expressed in (mmol m^{-2} day^{-1}). The gas transfer velocity k (m d^{-1}) strongly depends on water temperature and hydrodynamic conditions and was calculated using the widely accepted general equation Eq. (3) for N_2O (Wanninkhof, 2014):

$$k_{N2O} = k_{600} \times (Sc_t / 600)^{-n} \quad (3)$$

Where k_{600} is the normalized gas transfer velocity, and Sc_t is the Schmidt number of N_2O at in situ temperature, and 'n' is the Schmidt number exponent (0.5 cm h^{-1} for lakes, reservoirs, rivers and streams). Under hydrodynamic conditions, such as wind speed for standing waters (lakes, ponds, reservoirs) and velocity/channel slope for running waters (coastal/open oceans), this k_{600} was further determined as using the following Eq. (4):

$$k_{600} = 0.251 \times U_{10}^2 \times (Sc_t/600)^{-n} \quad (4)$$

Where 0.251 is an empirically determined constant used in the equation to relate wind speed to gas transfer velocity, and U_{10} is the wind speed at 10 meters above the water surface (in ms^{-1}). In eq (2), ΔC represents the concentration gradient, and H denotes Henry's law constant. The concentration gradient was calculated as the difference between the N_2O concentration in

https://doi.org/10.5194/essd-2026-109
Preprint. Discussion started: 13 May 2026

the water and the N_2O equilibrium concentration with the atmosphere, as, $\Delta C = (C_{water} - C_{eq})$.

This study compiled fluxes from diverse aquatic systems reported in the recorded publications (Data-source), and k values were adopted directly from the original publications whenever provided. When recalculations were necessary, k was assigned using system-specific ranges established in recent syntheses, with temperature normalization performed using the Schmidt number dependency with an exponent of -0.5.

Some studies additionally employed stable isotope labeling techniques to trace the sources and cycling of N_2O pathways, offering unique insights into its biogeochemical behavior and environmental impact, despite their relatively limited application. The integration of these approaches across GANED enhanced measurement accuracy and comprehensiveness, facilitating a deeper understanding of N_2O dynamics across diverse aquatic ecosystems.

2.3 Data standardization and quality assurance

Several steps were undertaken to assess the reliability and quality of the data compiled within GANED. This process included evaluating the accuracy of digitized data, followed by a series of additional verification procedures. Each data entry was cross-checked by a co-author other than the original contributor, when necessary. These checks encompassed validation of site details, variable units, and gas data entries, either through spot checks or full reviews, depending on the dataset size and whether the data were manually entered or imported from external files. After data entry, all gas and physicochemical variables were standardized to consistent units (Tables A3 and A4). Specifically, all concentrations were converted to ($\mu mol\ L^{-1}$) and fluxes to ($mmol\ m^{-2}\ day^{-1}$). Unit conversions employed standard molar volumes and gas constants; measurements originally reported in $nmol\ L^{-1}$, ppm or ppb were converted using Henry's law where appropriate. After converting all values to standard units, variables were visualized to detect irregularities, and any extreme values were cross-checked with the original data source. Unresolved records were excluded from the dataset, and missing data points for ancillary measurements or secondary metadata fields were explicitly denoted with 'NA' (Not Applicable/Not Available).

The quality control involved several steps: (1) cross-verification of units and values against original publications; (2) detection of irregularities detection using statistical thresholds (values >3 standard deviations from the mean per aquatic type were excluded, affecting <1% of entries); (3) handling of short data (having a single observation) in dataset files by noting limitations to ensure robustness in aggregated analyses; (4) assessment of measurement uncertainty, incorporation reported error ranges where available, for example, chamber-based flux measurements.

2.4 Uncertainty, plausibility assessment, and guidance for reuse

The GANED database integrates measurements compiled from 426 peer-reviewed studies across diverse aquatic environments, sampling designs, analytical methods, and reporting formats. Consequently, uncertainty in GANED arises from multiple sources, including heterogeneity in original measurement approaches, variation in temporal sampling frequency, incomplete reporting of ancillary variables, digitization of graphical information where tabulated values were unavailable, and differences in study-specific quality-control procedures. In addition, concentration measurements and direct flux observations are not always interchangeable, particularly in hydrologically dynamic systems, and this methodological heterogeneity should be

https://doi.org/10.5194/essd-2026-109
Preprint. Discussion started: 13 May 2026

considered when comparing records across aquatic types.

To reduce these uncertainties, we applied harmonized quality-assurance procedures during database construction, including standardized unit conversion, metadata harmonization, cross-checking of extracted values, removal of clearly implausible outliers, and explicit structuring of the database into source, site, concentration, and flux components.

A formal validation against an independent global reference product is currently not possible due to the lack of a globally consistent benchmark dataset for aquatic N_2O observations across all major water bodies. Instead, following ESSD principles, we provide a plausibility assessment based on internal consistency checks, cross-system comparisons, methodological evaluation, and explicit identification of underrepresented regions, ecosystems, and time periods.

Users should interpret GANED as a harmonized dataset product useful for comparison, meta-analysis, and hypothesis generation, while being aware of its representativeness limits. Notably, the spatial concentration records in Asia and North America, lack of long-term repeated observations, and the limited coverage of some transitional or intermittently connected aquatic systems may constrain global extrapolation and should be considered in downstream analyses.

2.5 Statistical Analysis

All data processing and analyses were conducted in R statistical software (version 4.5.1, R Core Team, 2025) using packages such as 'dplyr' (version 4.2; Wimberly (2023) and 'data.table' (Dowle and Srinivasan, 2023) for data manipulation, the "sf" package (version 4.2; Mishra et al., 2024) for spatial data handling, 'stats' for statistical analyses, and 'ggplot2' and 'patchwork' (version 4.2; Kabacoff; Thomer and Rayburn, 2024) for visualizations. Descriptive statistics (means, medians, standard deviations) were used to summarize the database, highlighting site distributions by country/continent and aquatic system type. Grouped means facilitated comparison of N_2O concentrations and fluxes across ecosystem categories. Temporal trends were assessed by aggregating observations into annual averages, followed by linear regression to identify changes from 1980 to 2023. To explore environmental drivers, correlation coefficients were calculated between N_2O fluxes and associated physiochemical variables, using pairwise complete observations to handle missing values. Statistical significance was denoted as *** for $p < 0.001$, ** for $p < 0.01$, and * for $p < 0.05$ for multiple comparisons.

3 Results

3.1 Introduction to the GANED

GANED comprised 5130 N_2O concentration records and 7386 N_2O flux records from 3002 unique sites spanning 1980-2023 (Fig. 3a). Notably, more than 85% of the concentration records and 80% of the flux measurements were published since 2015, with rivers and streams accounting for half of all observations (Fig. 3b). GANED revealed significant variation in N_2O emissions across different water body types, highlighting the growing significance of aquatic contribution to the global N_2O budget. As illustrated in Fig. 3b, rivers contribute the largest share (41.04%) of the total emissions, followed by lakes (13.02%), reservoirs (14.36%), and streams (8.43%), whereas seas and coastal areas contributed the least (2.63% and 1.53%, respectively)

https://doi.org/10.5194/essd-2026-109
Preprint. Discussion started: 13 May 2026

Open Access Earth System Science Data Discussions

despite their large surface area, contribute minimally to overall aquatic N_2O emissions. Long-term observations were rare, with only 2% (62/3002 sites; n = 62) having more than 10 concentration observations (total=1629 observational counts), and 4% (130/3002 sites; n = 130) having more than 10 flux records (total=3807 counts). Among these sites, observation counts ranged from 13 to >100 per site. The longest concentration record spans 11 years (Priscu et al., 2008), whereas the longest flux record spanned 19 years (De Wilde and De Bie, 2000).

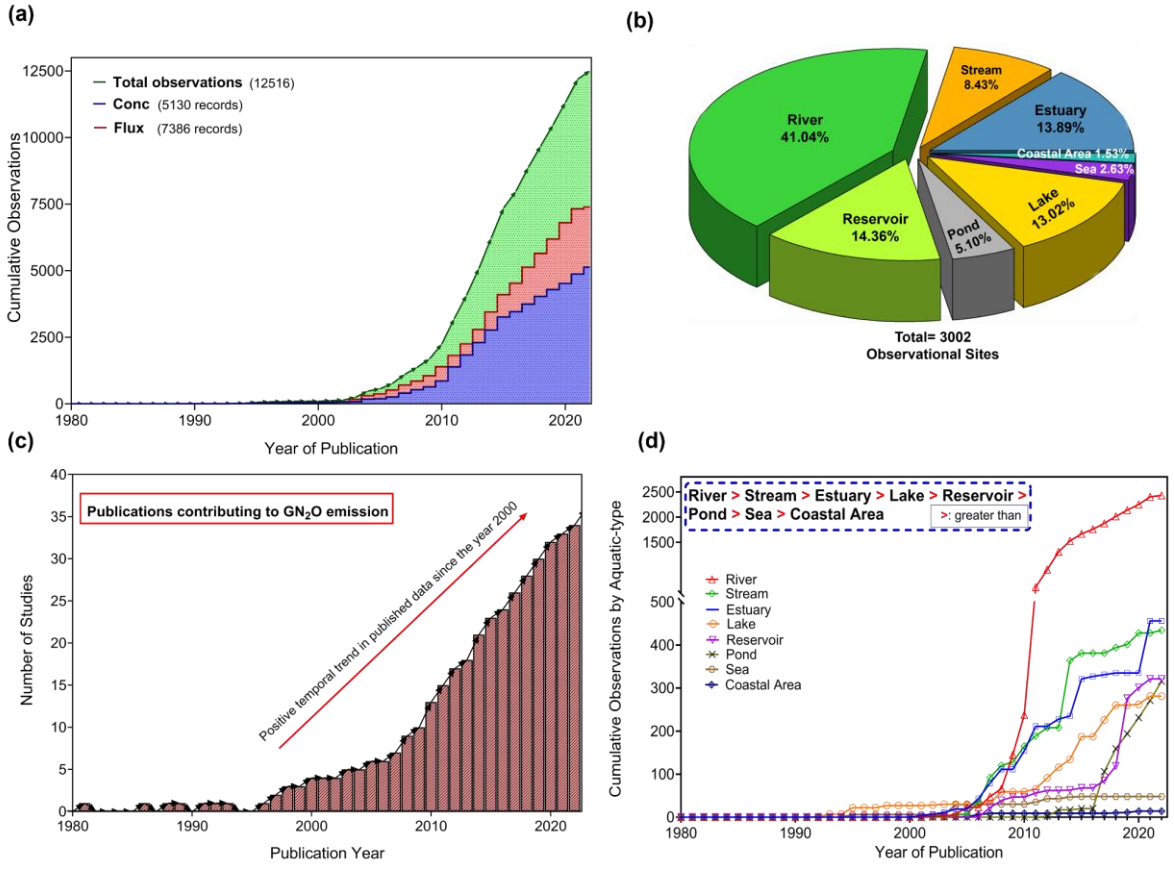

Figure 3: Global N_2O emissions (concentration and flux) from aquatic bodies over time, (a) cumulative observations of N_2O concentration and flux data, (b) proportion of water bodies contributions to net N_2O emission, (c) publications contributing to global N_2O emission, (d) the number of cumulative observations showing emission trends across different aquatic types over time.

Spatially, the majority of N_2O observations were concentrated in Asia (60%), followed by North America, which accounted for 15% of total N_2O observational sites. Europe, Oceania, and Africa had moderate but meaningful contributions compared to Asia and North America. In contrast, areas with extensive inland and coastal water bodies, such as Antarctica, Central America, and South America, were sparsely represented or entirely lacking observations, highlighting persistent geographical biases in global N_2O monitoring (Fig. 4). The heterogeneous distribution of observations underscored both the global relevance and uneven coverage of aquatic N_2O studies, offering important insights into spatial variability of concentrations and fluxes

https://doi.org/10.5194/essd-2026-109
Preprint. Discussion started: 13 May 2026

Open Access Earth System Science Data Discussions

across diverse water bodies. Further, number of observations for all variables by continent are shown in (Table S5).

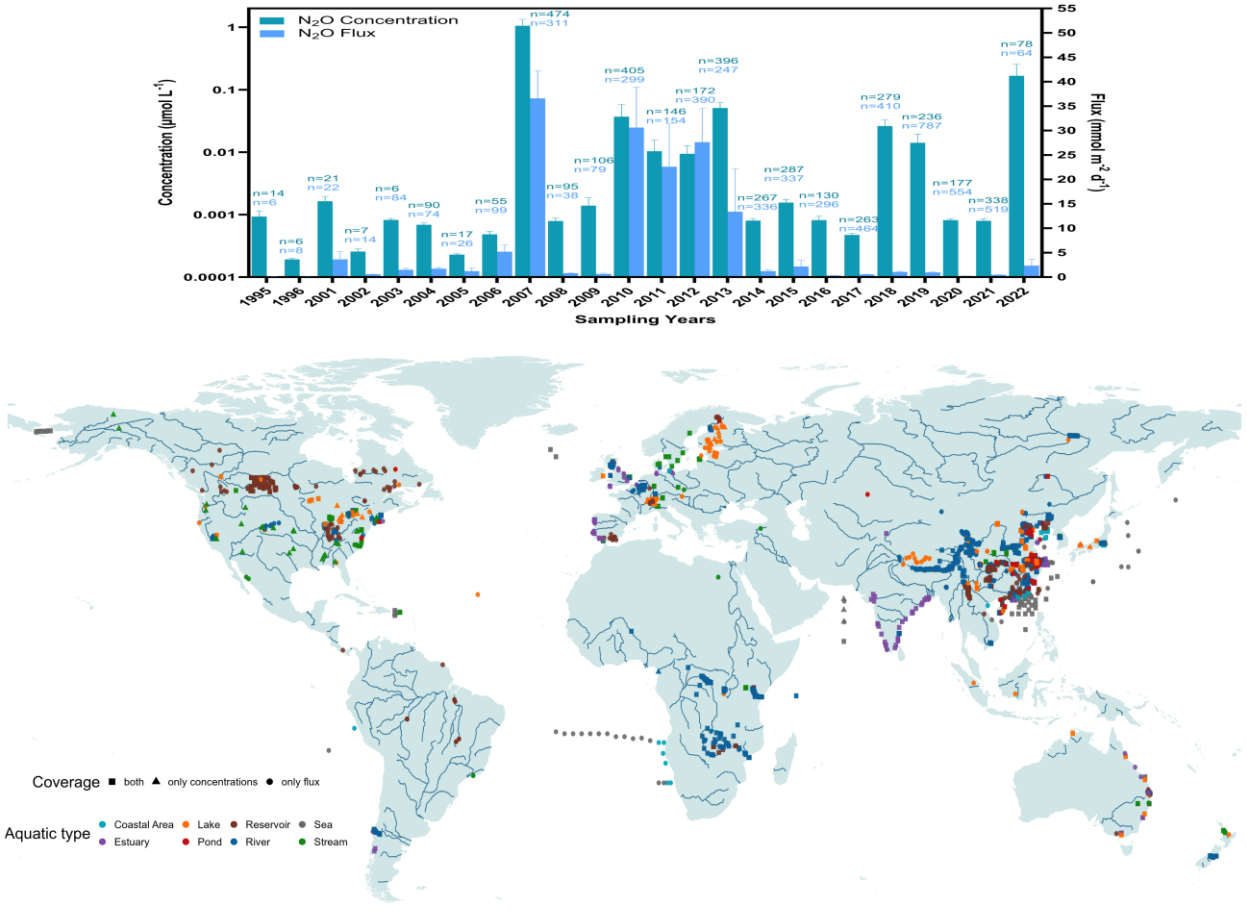

335 **Figure 4: Global distribution of N_2O observations in the database. Different symbols on the map represent observational sites where N_2O emissions were observed, categorized by the type of aquatic system (e.g., River, Stream, Lake, Estuary, Reservoir, Pond, Sea, and Coastal Area). The color coding identifies the type of aquatic type, while the shape and color of each symbol indicate whether the measurements focus on N_2O concentration, flux data or both.**

The temporal distribution of N_2O concentration (a) and flux (b) measurements across various aquatic types has been illustrated
340 in Fig. 5. The observational data revealed a clear latitudinal gradient, with an increasing number of studies over time. Prior to 2000, concentration records were largely restricted to the Northern Hemisphere (30°-60°N), mainly across North America, Europe, and eastern Asia, reflecting the early focus on temperate mid-latitudes (Fig. 5a). After 2000, observations expanded across the Southern Hemisphere and tropics, achieving near-global coverage by 2010-2020, with notably accelerated records in South America, sub-Saharan Africa, Southeast Asia, and Australia. Recent measurements (2010-2020; yellow/red symbols)
345 from tropical estuaries and rivers (10°S-30°N), notably in Southeast Asia and the Amazon Basin, frequently reported the highest N_2O concentrations.

The corresponding flux data followed similar temporal trends in sampling distribution consistent with the concentration data

https://doi.org/10.5194/essd-2026-109
Preprint. Discussion started: 13 May 2026

Open Access Earth System Science Data Discussions

(Fig. 5b). Early fluxes (1980-2000) were concentrated in mid-latitude regions, whereas more recent flux observations (2010-2020) were frequently reported within tropical zones (15°S-15°N), particularly in estuaries, rivers, and reservoirs across Southeast Asia, eastern China, India, and South America. Flux observations were also evident in Southern Hemisphere subtropical regions. Overall, rivers and streams consistently exhibited high fluxes across latitudes, with the most pronounced emissions occurring in tropical and subtropical systems, emphasizing their critical role as persistent aquatic N_2O sources.

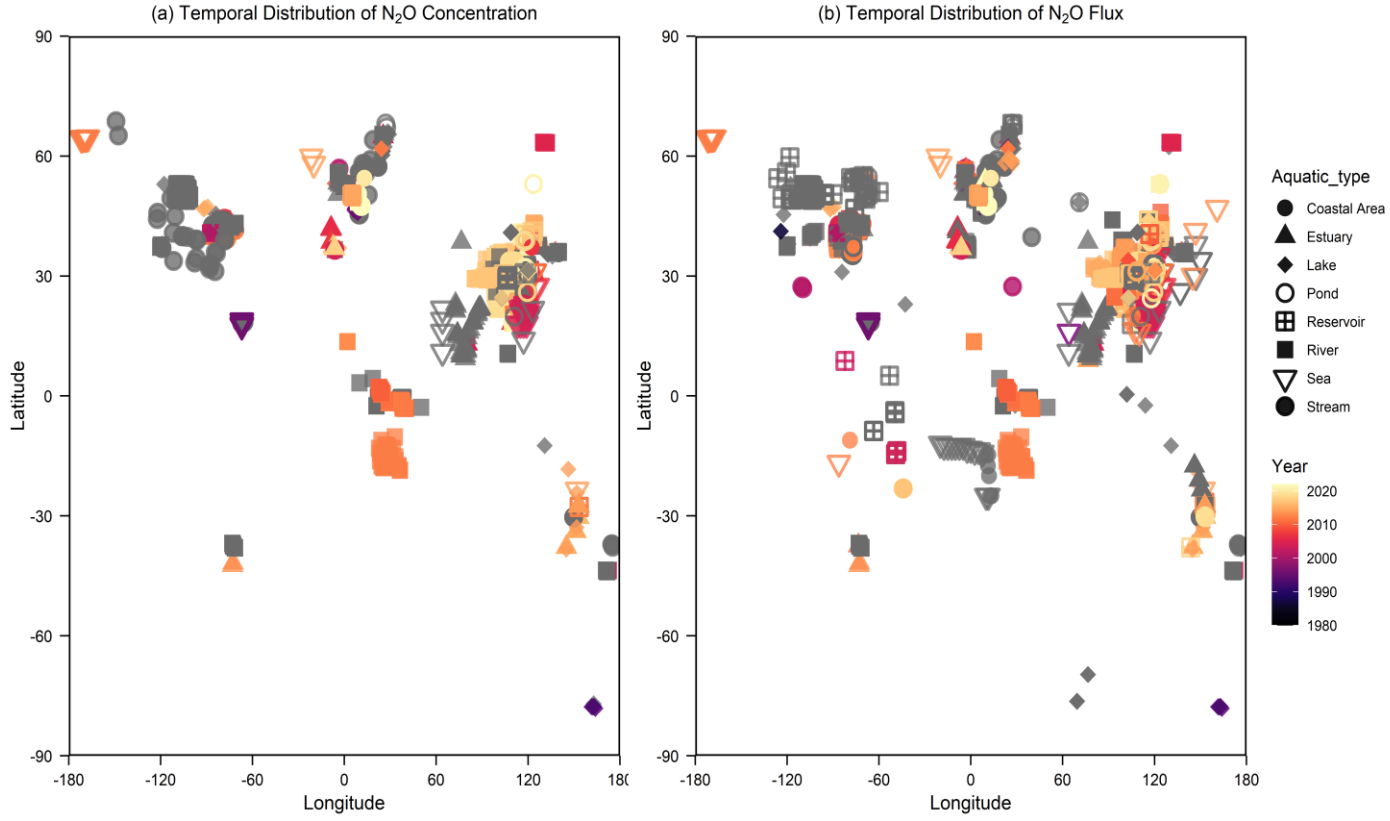

Figure 5: Temporal distribution of N_2O emissions across different aquatic types over the years, (a) temporal distribution of N_2O concentration (left), with data points color-coded by years, ranging from 1980 (purple) to 2020 (yellow/red), and (b) temporal distribution of N_2O flux (right) across longitude and latitude coordinates over same period of time.

Temporally, long-term trends in mean N_2O concentrations across aquatic types varied substantially (Fig. 6). Rivers and streams generally exhibited the highest concentrations and greatest interannual variability. Rivers showed extreme fluctuations, with mean concentrations occasionally exceeding 1.0 (on the $\log_{10}$ scale), though no definitive long-term linear trend was evident due to high variability. Streams, however, displayed a distinct increasing trend in N_2O concentration, particularly notable from 2010 onward. Lakes and ponds exhibited a sharp decrease following a peak around 2011. Transitional and marine systems, such as estuaries, reservoirs, seas, and coastal areas, were characterized by the lowest overall N_2O concentrations, generally remaining stable or showing only marginal increasing trends over the decades.

https://doi.org/10.5194/essd-2026-109
Preprint. Discussion started: 13 May 2026

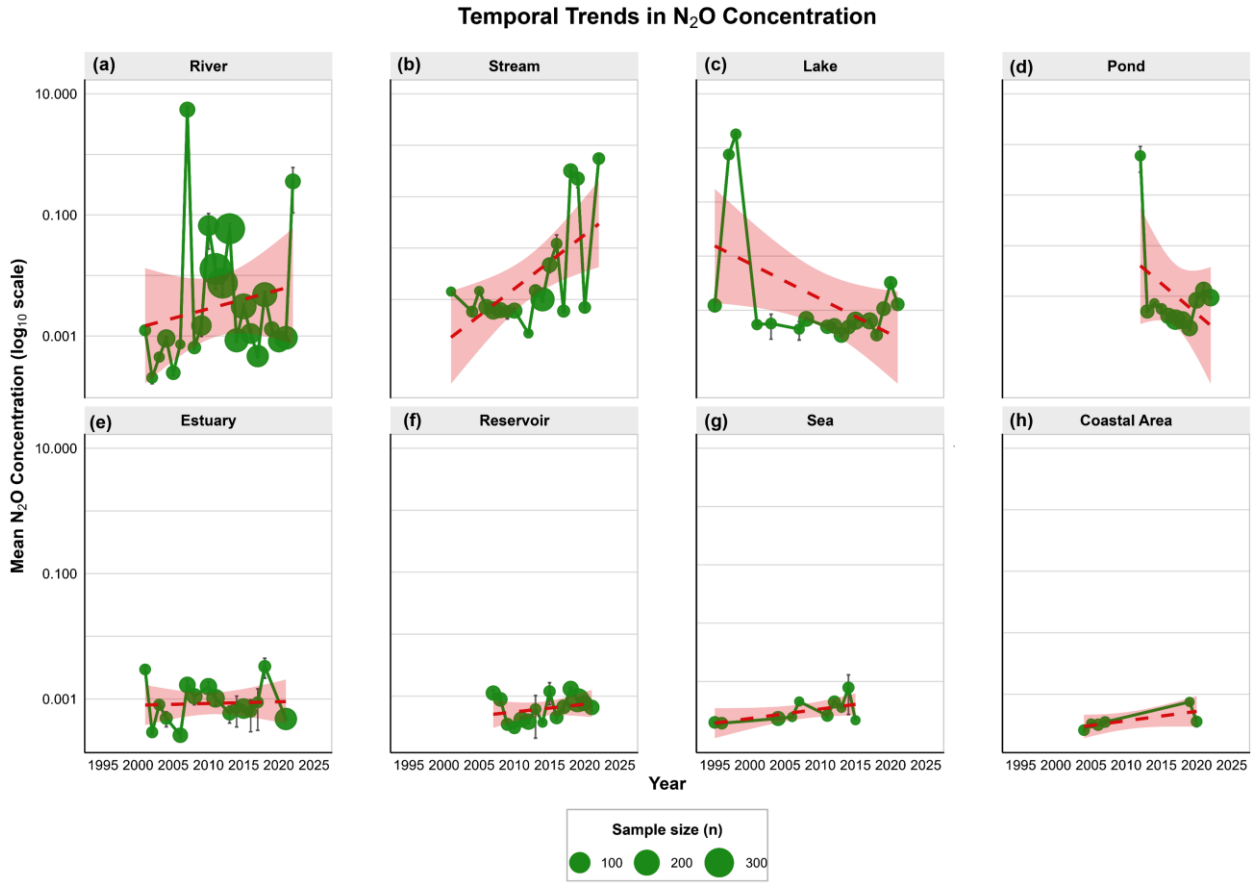

Figure 6: Temporal trends in mean dissolved N_2O concentration (log_{10} scale) across aquatic types: (a) River, (b) Stream, (c) Lake, (d) Pond, (e) Estuary, (f) Reservoir, (g) Sea, and (h) Coastal Area. Green dots represent annual means concentration with circle size proportional to sample size (n= 100, 200, 300); pink shading and red line show the loess-smoothed trend with 95% confidence interval. Vertical error bars indicate standard error. Subplots are arranged in two rows with a shared y-axis per row to facilitate comparison.

Temporal trends in mean N_2O fluxes were highly dependent on aquatic type and characterized by significant temporal heterogeneity and episodic high-emission events (Fig. 7). Rivers dominated emission magnitudes, driven by extreme episodic peaks, ~200 mmol m^{-2} d^{-1}. Despite these peaks, the overall trend line for rivers suggested a slight decrease or stabilization in recent years. Streams, lakes, ponds, and estuaries generally exhibited decreasing trends in mean N_2O flux over the observed period, despite the increasing concentrations noted in streams in Fig. 6. Lakes and reservoirs were characterized by generally low baseline fluxes punctuated by singular, intense emission years, e.g., the Lake peak in 2011. Seas generally reported low and stable flux rates. Coastal areas showed a marked increasing trend in emissions, although data availability for this specific category was limited to the period prior to 2015.

https://doi.org/10.5194/essd-2026-109
Preprint. Discussion started: 13 May 2026

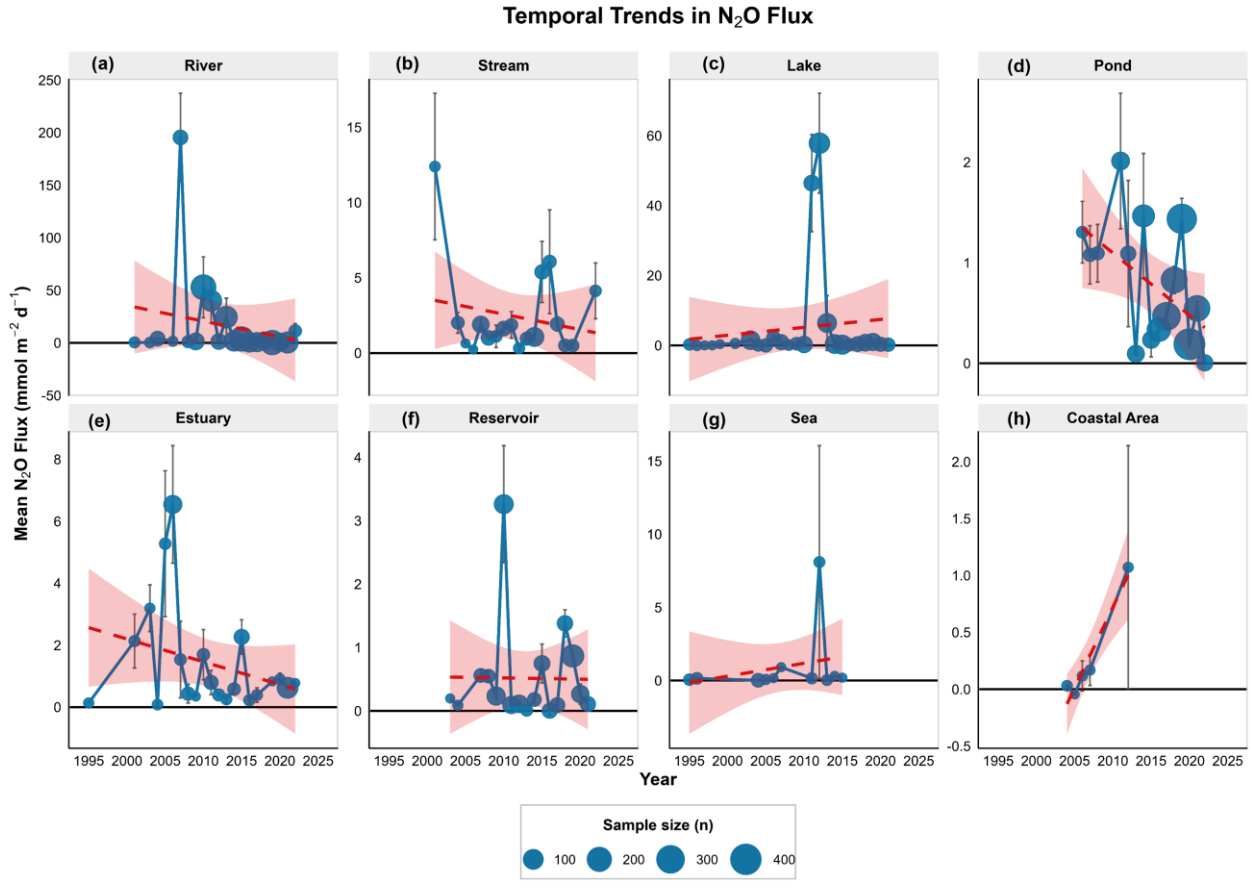

Figure 7: Temporal trends in mean N_2O flux (mmol m^{-2} d^{-1}) across aquatic types: (a) River, (b) Stream, (c) Lake, (d) Pond, (e) Estuary, (f) Reservoir, (g) Sea, and (h) Coastal Area. Blue dots represent annual mean fluxes; pink shading and red line show the loess-smoothed trend with 95% confidence interval. Dot size is proportional to the sample size in each year (100-400). Vertical error bars indicate standard error.

3.2 Distribution patterns of N_2O concentrations and fluxes

The distributions of observed N_2O concentrations and fluxes in GANED were strongly positively skewed, with the majority of the data being collected predominantly occurring in the Northern Hemisphere (Fig. 8). Most concentration measurements ranged between 10^{-4} and 10^{-3} µmol L^{-1} (Fig. 8a), with rivers and streams contributing the largest share of observations within this interval. Isolated but exceptionally high concentrations (> 400 µmol L^{-1}) were recorded, reflecting the presence of intense local emission hotspots (Sun et al., 2009). N_2O fluxes displayed a similar pattern, spanning from -9.3 to 164 mmol m^{-2} d^{-1}, with ~500 observations falling between 10^{-2} and 10^{0} mmol m^{-2} d^{-1} (Fig. 8b). Approximately 13% of reported fluxes were zero, below detection limits, or negative, emphasizing the inherent variability and uncertainty associated with flux measurements across diverse aquatic environments.

Latitudinal patterns provided additional insight into the distribution of concentration and flux observations across climatic zones and revealed substantial spatial heterogeneity and sampling bias (Fig. 8c,d). Data coverage was heavily concentrated in

https://doi.org/10.5194/essd-2026-109
Preprint. Discussion started: 13 May 2026


Open Access Earth System Science Data Discussions

the Northern Hemisphere, particularly within subtropical and temperate regions between 20°N and 60°N. This latitudinal band not only contained the majority of sampling efforts but also exhibits the highest emission magnitudes. Within this dominant Northern Hemisphere region, the temperate zone (~40°N-60°N) showed dense clustering of data, primarily from rivers, lakes, and reservoirs, with concentrations generally centered around 10^{-2} μmol L^{-1}. However, the subtropical zone (20°N-40°N) displayed the highest variability. Rivers, streams, lakes, and reservoirs in these regions not only accounted for the majority of available observations but also produced the most substantial emissions, highlighting their role as major global hotspot of aquatic N_2O emission.

In contrast, the tropical zone (from the equator to ~23.5° N/S) and the entire Southern Hemisphere were characterized by sparse observational data coverage. Although localized elevated concentrations occurred in tropical rivers and reservoirs near the equator (0°), their frequency and peak magnitudes were substantially lower than those recorded in the northern subtropics. High-latitude systems, including boreal and polar regions beyond 60°N and much of the area south of 40°S, were similarly underrepresented across all aquatic ecosystem types. Overall, rivers, streams, and lakes in the northern subtropical and temperate bands continued to dominate current knowledge of high aquatic N_2O emissions, while pronounced data gaps persist for tropical and Southern Hemisphere regions.

More than 80 % of all measurements originated from high-income and upper-middle-income economies (World Bank classification, 2024), with the top five contributing countries, China ~38 %, United States ~15 %, Germany ~8 %, India ~5 %, and United Kingdom ~4 %, accounting for ~70 % of the entire dataset. China alone contributes the majority of extreme hotspots (Concentration: >50 μmol L^{-1} and flux: >100 mmol m^{-2} d^{-1}), reflecting intense sampling effort in the heavily fertilized Yangtze, Yellow River, and Hai River basins and southeastern coastal provinces. The United States showed a similar pattern in the Mississippi River basin and Midwestern agricultural states. In contrast, low-income and lower-middle-income countries together contributed <6 % of records, of which these observations were largely restricted to a small number of major river systems such as the Congo, Amazon, and Ganges-Brahmaputra.

https://doi.org/10.5194/essd-2026-109
Preprint. Discussion started: 13 May 2026

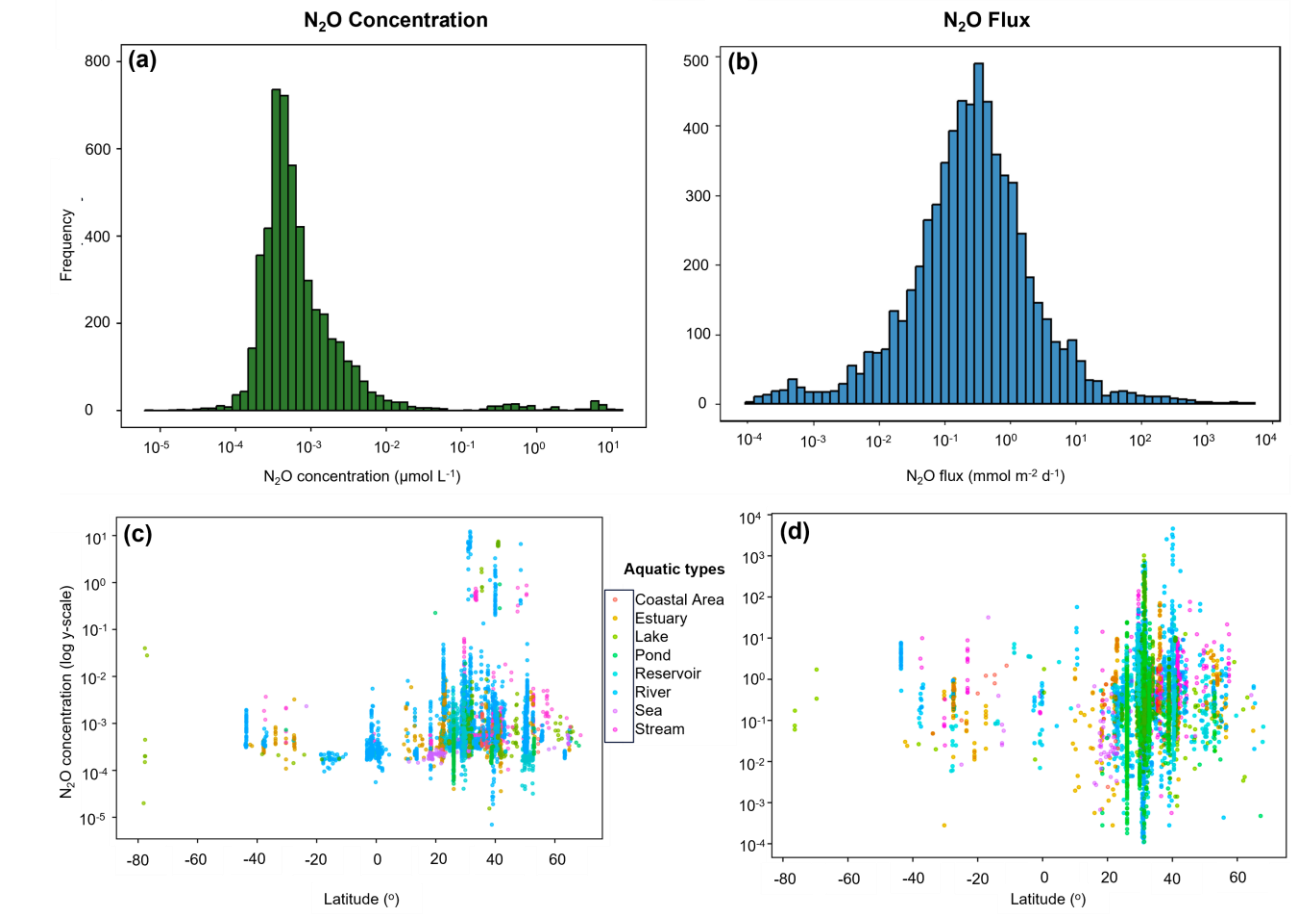

Figure 8: Distribution of N_2O concentrations and fluxes across different aquatic types, derived from the GANED. (a,b) represent frequency histograms of N_2O concentrations (μmol L^{-1}) and fluxes (mmol m^{-2} d^{-1}), respectively. (c,d) display the latitudinal distribution of N_2O concentrations (left) and fluxes (right) on a log scale. Different colors of observations denote the distinct aquatic type.

3.3 Statistical overview of N_2O concentration and flux by aquatic types

Statistical summaries of N_2O concentrations and fluxes in the GANED dataset by aquatic ecosystem types revealed marked differences in central tendencies and extreme values (Table S2). Lakes exhibited the highest mean dissolved N_2O concentration, 0.406 μmol L^{-1}, followed by rivers, 0.077 μmol L^{-1}, and streams 0.029 μmol L^{-1}. Rivers also recorded the highest maximum concentration with 12.23 μmol L^{-1}. In contrast, ponds, estuaries, coastal waters, and seas generally showed low concentrations, with median values frequently at or near zero and maximum values consistently below 0.011 μmol L^{-1} (Table S3).

For N_2O fluxes, rivers displayed both the highest mean flux, 15.45 mmol m^{-2} d^{-1} followed by lakes, 10.34 mmol m^{-2} d^{-1}, and streams 3.75 mmol m^{-2} d^{-1}, respectively. Estuaries, reservoirs, coastal waters, and seas exhibited substantially lower mean fluxes (all < 1 mmol m^{-2} d^{-1}) and accounted for the majority of zero or negative values, indicating these systems often functioned near equilibrium or as weak N_2O sinks (Table S4). Furthermore, summary statistics for concurrently measured

https://doi.org/10.5194/essd-2026-109
Preprint. Discussion started: 13 May 2026

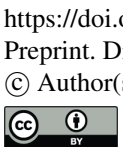

Open Access Earth System Science Data Discussions

GHGs (CO_2 and CH_4) concentrations and fluxes are provided in Table S1 and Fig. S1.

Boxplot analysis of N_2O concentrations and fluxes across different aquatic types in the GANED dataset highlighted significant variability and distinct emission profiles, with sample sizes denoted below each aquatic category (Fig. 9). For N_2O concentrations (Fig. 9a), rivers exhibited the widest interquartile range (IQR) and the highest median value on a logarithmic scale, reflecting their role as primary emission hotspots. Streams and lakes displayed moderate medians and IQRs, while ponds, estuaries, reservoirs, coastal areas, and seas exhibited progressively lower medians. Seas had the lowest median concentration, consistent with their limited number of observations (n = 58). The pronounced scattering of outliers, particularly in rivers and streams, further highlighted the influence of localized nutrient enrichment and key biogeochemical processes such as nitrification and denitrification.

Correspondingly, for N_2O fluxes, rivers and ponds emerged as prominent emission hotspots, exhibiting the greatest magnitude and variability in fluxes, with broader outliers accounting for 1685 and 2173 observations, respectively (Fig. 9b). Lakes and estuaries exhibited intermediate flux levels, whereas seas and coastal waters consistently displayed the lowest N_2O flux values.

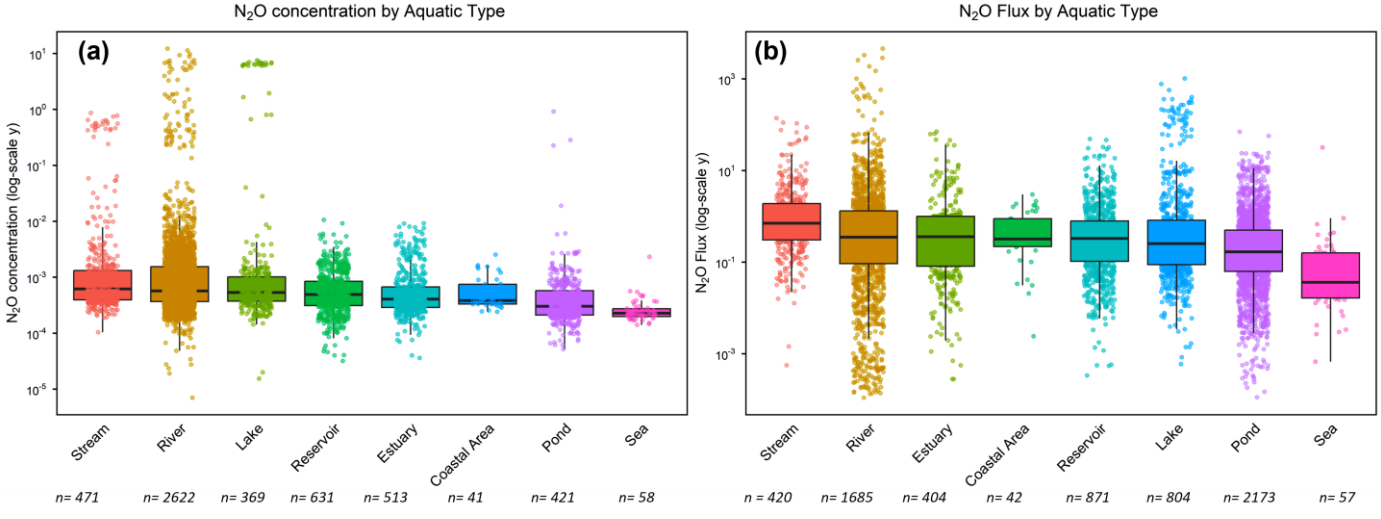

Figure 9: N_2O concentration and flux across aquatic types. Data was derived from the GANED, comprising 5,126 concentration records and 6456 flux measurements. Boxplots representing the median (central line), interquartile range (box), and data range (whiskers) of distribution of dissolved N_2O concentration (left), and N_2O flux (right) across different aquatic types. Missing or NA values were omitted.

3.4 N_2O flux dynamics and environmental predictors

The relationships between N_2O fluxes and key environmental drivers were examined using correlation analyses, revealing significant associations that highlighted the underlying biogeochemical controls on N_2O emissions from aquatic bodies (Fig. 10). NH_4^+ exhibited a strong positive correlation with N_2O fluxes ($R^2 = 0.889$, $p < 0.001$), emphasizing the role of reduced N availability in driving N_2O emissions, potentially via nitrification or coupled nitrifier denitrification. NO_3^- also showed a

https://doi.org/10.5194/essd-2026-109
Preprint. Discussion started: 13 May 2026

significant positive relationship (R^2 = 0.477, p < 0.001), underscoring the contribution of oxidized inorganic N as a substrate for N_2O production. DOC displayed a moderate positive correlation, consistent with its role in providing electron donors for heterotrophic processes such as denitrification. In aquatic systems, the DOC: NO_3^- ratio is frequently used to indicate the preferred pathway of NO_3^- reduction, with higher ratios favoring complete or incomplete denitrification, which can produce N_2O as an intermediate over assimilatory uptake or dissimilatory reduction to ammonium (DNRA). The positive association observed here with both DOC and inorganic N species (NH_4^+, NO_3^-, NO_2^-) suggested that denitrification likely contributed substantially to N_2O fluxes in these systems, particularly under conditions of sufficient organic carbon availability. In contrast, TP had a weak negative correlation (R^2 = 0.148, p = 0.614), indicating a limited influence on N_2O fluxes. DO displayed a negative correlation (R^2 = 0.042, p = 0.048), suggesting that lower oxygen levels and cooler temperatures may favor denitrification processes. Similarly, water temperature exhibited an inverse relationship with N_2O fluxes (R^2 = 0.469, p = 0.012). Salinity showed a moderate correlation (R^2 = 0.404, p = 0.005; R^2 = 0.063, p = 0.206), whereas TN had a negligible non-significant effect (R^2 = 0.63, p = 0.206). Additional quantitative results for all analyzed predictors are provided in (Table 2) and summary statistics in (Table S6).

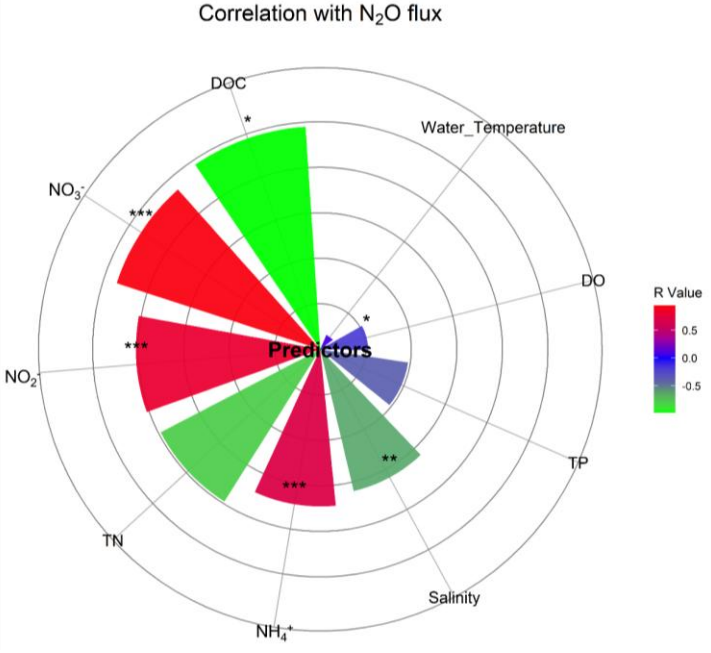

Figure 10: Radial correlation plot depicting the relationships between N_2O fluxes and key environmental predictors. The correlation strengths (R^2 values) are shown with color gradients (red to green indicating positive to negative associations) at significance levels (* p < 0.001, ** p < 0.01, * p < 0.05).**

https://doi.org/10.5194/essd-2026-109
Preprint. Discussion started: 13 May 2026

Table 2: Linear regression models based on the parable portion of the data (approximately 190 rows with non-NA N_2O-Flux values after filtering). The R value is the Pearson correlation coefficient, R^2 obtained as $R^2 = (R\text{-value})^2$, and significance is based on the *p*-value (* for $p < 0.001$, ** for $p < 0.01$, * for $p < 0.05$).**

Predictors	Slope	Intercept	R Value	R^2 Value	P Value	Std. Error	Significance
NH_4^+	3.318	-0.160	0.943	0.889	5.11×10^{-11}	0.262	***
NO_2^-	16.179	-0.677	0.807	0.651	5.65×10^{-6}	2.647	***
NO_3^-	3.738	-1.674	0.691	0.477	3.68×10^{-6}	0.874	***
Salinity	-0.181	5.024	-0.636	0.404	0.005	0.055	**
DO	-0.131	1.379	-0.205	0.042	0.048	0.065	*
DOC	-0.261	1.131	-0.977	0.955	0.023	0.040	*
Water-Temperature	0.012	0.297	0.070	0.004	0.469	0.017	Ns
TP	-0.002	0.301	-0.386	0.148	0.614	0.003	Ns
TN	-0.413	1.136	-0.794	0.630	0.206	0.224	Ns

Note: pH (excluded) had insufficient non-NA pairwise data for regression in the recorded N_2O flux observations.

Furthermore, using a machine learning (ML) approach, the predictive performance of the random forest (RF) model of ML for estimating N_2O flux across all aquatic types combined in GANED was analyzed and complemented by feature importance analysis. The model was trained on a dataset with an 80% training and 20% testing split, and performance was evaluated using root mean square error (RMSE), mean absolute error (MAE), and the coefficient of determination (R^2), with RF demonstrating robust predictive capability despite the inherent variability in global N_2O flux data. RMSE = 84.41, MAE = 6.96, and R^2 = 0.13 values for RF indicated the explained variance in the N_2O flux data. The permutation feature importance results from the RF model, expressed as percentage increase in mean squared error (%IncMSE) when each feature was randomly permuted (Fig. 11), identified NO_3^- as the dominant predictor with a value of 23.60%, followed by NH_4^+,15.74%; DO, 11.39%, and NO_2^-, 7.85%. The remaining environmental predictors showed lower but notable contributions: TN, 5.39%; pH, 5.12%; water temperature, 4.82%; DOC, 4.73%; TP, 3.65%, and salinity, 2.61%.

https://doi.org/10.5194/essd-2026-109
Preprint. Discussion started: 13 May 2026

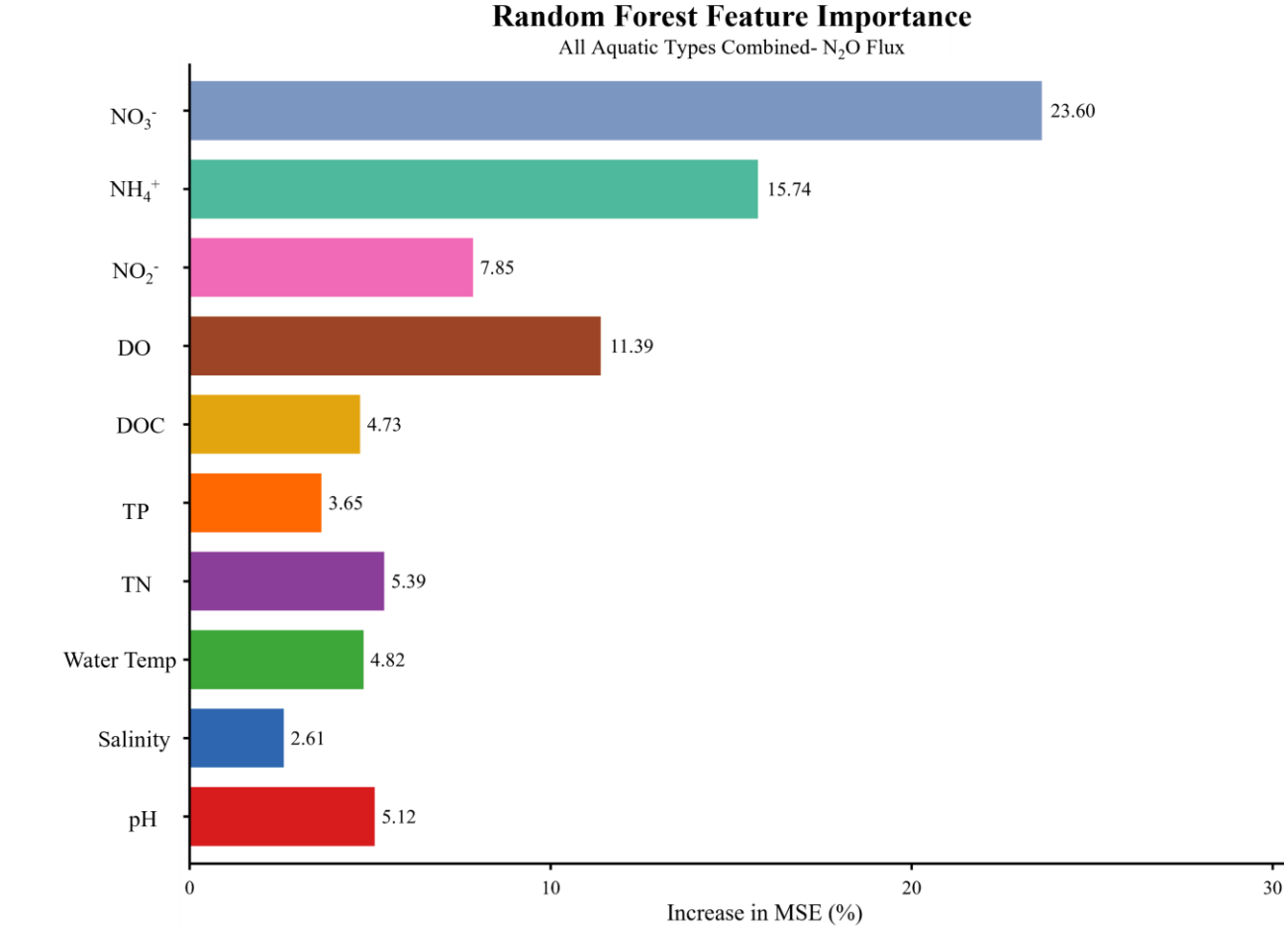

Figure 11: Feature importance of environmental predictors in the RF model for N_2O flux. The bar chart shows the increase percentage in Mean Squared Error (IncMSE%) for each environmental predictor, with a higher percentage (%) indicating greater predictive importance for N_2O flux.

To further unravel the controls on N_2O emissions across different water bodies in GANED, we conducted individual RF models for each aquatic type using only samples with complete data for all predictors (Fig. S2). Model performance varied considerably due to differences in sample size, data variability, and inherent emission ranges (Table 3). Lakes showed the highest $R^2 = 0.2424$, followed by estuaries $R^2 = 0.2250$, and ponds $R^2 = 0.1817$, respectively. Marine systems, seas and coastal areas, exhibited negative R^2 values, indicating poor predictive skill, likely due to very low sample sizes, n=70 and n=49, respectively, and limited variability in emissions.

Permutation-based feature importance, expressed as IncMSE%, revealed marked heterogeneity in the dominant controls on N_2O flux across aquatic types. In rivers, NO_3^-: 32.97% and NH_4^+: 21.60%, together accounted for >50% of predictive importance, with DO and water temperature contributing substantially, ~15% each. Streams were primarily governed by water temperature = 20.22%, and DO = 19.69%, followed by TP and NO_3^-. Ponds, the most data-rich lentic system, showed NH_4^+

https://doi.org/10.5194/essd-2026-109
Preprint. Discussion started: 13 May 2026

=16.0% as the leading predictor, closely followed by NO_2^-, temperature, and TN= ~12% each. In reservoirs, salinity emerged as the top predictor, accounting for 16.83% of IncMSE%, ahead of NO_3^-=14.58% and pH, 11.2%. Estuaries exhibited strong influence of DO,17.62%; NO_3^-, 15.38%; water temperature,14.54%; and NH_4^+, 14.32%. Lakes displayed the most balanced importance distribution, with pH, 5.86%, and TN, 5.21%, marginally leading and no single predictor exceeding 6%. Marine systems (sea, n = 70; coastal area, n = 49) yielded unreliable importance rankings due to insufficient sample size and low emission variability.

Table 3: Random Forest (RF) model performance and permutation feature importance (% increase in MSE) for predicting N_2O flux by aquatic type in GANED. Types ordered by number of complete cases. Feature importance values rounded to one decimal place

Aquatic type	n	R^2	Top predictors Feature Importance (% IncMSE)
River	1830	0.120	NO_3^- (32.97%), NH_4^+ (21.60%), DO (14.74%), Temp. (14.22%)
Stream	431	0.090	Temp. (20.22%), DO (19.69%), TP (15.09%), NO_3^- (14.97%)
Pond	2476	0.182	NH_4^+ (16.0%), NO_2^- (12.23%), Temp. (12.08%), TN (11.67%)
Reservoir	1119	0.170	Sal. (16.83%), NO_3^- (14.58%), pH (11.2%), TN (11.06%)
Estuary	438	0.225	DO (17.62%), NO_3^- (15.38%), Temp. (14.54%), NH_4^+ (14.32%)
Lake	973	0.242	pH (5.86%), TN (5.21%), TP (3.46%), NH_4^+ (3.44%)
Sea	70	-0.017	Limited reliability (low n)
Coastal area	49	-0.099	Limited reliability (low n)

4 Discussion

The magnitude and heterogeneity of N_2O emissions from global aquatic bodies remain challenging to quantify, largely due to the fragmented nature of existing observations and pronounced spatiotemporal inconsistency of available flux measurements (Song et al., 2024). The GANED database represents the most comprehensive observation-based synthesis of aquatic N_2O concentrations and fluxes, enabling a mechanistic interpretation of emission patterns across different water-body types rather than treating aquatic environments as a uniform source. As a global compilation, its main contribution is to make previously fragmented N_2O concentration and flux observations more accessible, comparable, and reusable through standardized structure, metadata linkage, and quality assurance. By integrating 7,386 flux measurements and 5,130 concentration records, this study elucidates that N_2O emission dynamics are strongly system-specific and primarily controlled by substrate availability. We also discuss the main features of the compiled dataset, its heterogeneity, its current coverage gaps, and the implications for future reuse and synthesis.

4.1 Aquatic ecosystems as heterogeneous N_2O observation domains

https://doi.org/10.5194/essd-2026-109
Preprint. Discussion started: 13 May 2026

The GANED highlights that aquatic N_2O observations are distributed across strongly contrasting aquatic settings, including flowing inland waters, standing waters, estuarine systems, and marine environments. The dataset shows substantial variation in the magnitude and spread of reported concentrations and fluxes among these aquatic types, indicating that global aquatic N_2O observations should not be treated as a uniform data class. For data users, this heterogeneity is an important feature of the compilation because it supports cross-system comparison while also indicating that aquatic type, sampling context, and methodological differences should be considered explicitly in synthesis, model evaluation, and comparative analyses. The highly right-skewed distributions of both N_2O concentrations and fluxes (Fig. 8) constitute a central outcome of GANED, confirming that rivers, streams, ponds, and certain lakes exhibit higher and more variable per-area N_2O fluxes. In contrast, open seas are characterized by marginal fluxes close to zero, and by a substantial occurrence of negative fluxes (approximately 13% of observations), highlighting their episodic role as N_2O sinks (Ansari et al., 2024). The elevated fluxes observed in nutrient-enriched rivers and streams can be attributed to distinct aquatic process controls, including direct N loading (Tonina et al., 2021) and rapid microbial turnover in hyporheic zones and sediments (Yan et al., 2024). These processes often produce per-unit-area N_2O emissions that exceed those of many terrestrial soils, though driven by fundamentally different biogeochemical mechanisms. Importantly, recent evidence has indicated that low-order streams and headwaters often contribute disproportionately to N_2O emissions relative to larger rivers, a pattern linked to their high surface-area-to-volume ratios, shorter water residence times, and stronger coupling between sediments and the overlying water column (Marzadri et al., 2021; Hall Jr and Ulseth, 2020).

Our statistical analysis supports a predominantly substrate-driven control mechanism for aquatic N_2O emissions. In rivers and streams, NO_3^- and NH_4^+ together account for more than 50% of RF predictive importance, indicating the co-occurrence of nitrification in aerobic sediment surfaces, denitrification within hypoxic microsites, and nitrifier-denitrification under elevated NH_4^+ conditions (Lu et al., 2023). This mechanistic framework explains the wide distribution of riverine fluxes, particularly at sites influenced by point-source effluent or agricultural drainage, rather than implying that rivers act as persistently high N_2O emitters. GANED further reveals intermediate yet episodic flux behavior in lakes and estuaries, driven by denitrification, transient re-oxygenation pulses, and incomplete reduction of N_2O during turnover events (He et al., 2023; Liu et al., 2025). Ponds exhibit disproportionately high per-area emissions due to high surface-area-to-volume ratios, organic-rich sediments, and frequent anoxia conditions coupled with redox oscillation. In the RF model, emissions in ponds were primarily regulated by NH_4^+, NO_2^-, and temperature, consistent with intense nitrifier-denitrification at shallow benthic interfaces (Yang et al., 2020). In contrast, seas and coastal waters display low per-area and less variable fluxes, as N_2O production is distributed over large water volumes and oxygen-deficient zones occupy only limited spatial extents (Wang et al., 2025). The comparatively low predictive power of the RF model for these water bodies primarily reflects both limited sample sizes and intrinsically low flux variance, underscoring the need for improved database synthesis to better constrain marine N_2O emission potential, particularly within data-poor oxygen-deficient zones (Rees et al., 2022).

4.2 Spatiotemporal coverage, data biases, and remaining gaps

https://doi.org/10.5194/essd-2026-109
Preprint. Discussion started: 13 May 2026

The database shows that the number of published aquatic N_2O observations has increased substantially since 2000 (Fig. 3), but the spatial and temporal distribution of records remains uneven. Understanding the spatial and temporal variability in N_2O concentrations and fluxes across aquatic bodies is essential for improving global emission models. Given the high global warming potential of N_2O, robust quantification of emissions from diverse aquatic bodies, from rivers and lakes to open seas and coastal waters, is critical for reliable climate assessments. Over the past decade, research on aquatic N_2O emissions has undergone significant spatial expansion. A large fraction of sites is concentrated in Asia and North America, whereas Africa, South America, and high-latitude regions remain comparatively underrepresented (Stanley et al., 2022). Temporal continuity is also limited, with relatively few sites containing long-term repeated observations. Although these gaps do not diminish the intrinsic value of GANED as a synthesis product, they establish critical constraints on representativeness that must be considered for regional comparison, global extrapolation, or gap-filling.

GANED highlights both the global significance of emission hotspots and the potential underestimation associated with limited spatiotemporal sampling. Our analysis reveals pronounced spatial bias in existing N_2O observations, with more than 60% of observational sites located in Asia, predominantly reflecting concentrated research efforts in East Asia. This is consistent with the regions having high anthropogenic N input and dense hydrological monitoring networks (Tian et al., 2024; Wang et al., 2023). Conversely, large areas of Africa, South America, and high-latitude regions remain sparsely monitored (Fig. 4), creating substantial blind spots in global upscaling efforts. Such spatial inequity mirrors gaps identified in other global GHG databases (Rosentreter et al., 2021) and accentuates the risk of bias towards temperate and subtropical aquatic systems, while underrepresenting tropical and polar aquatic fluxes, which may exhibit distinct biogeochemical dynamics for N_2O production (Lauerwald et al., 2025).

The spatial distributions of N_2O emission, as described in Sect. 3.1, display strong latitudinal clustering within subtropical to temperate regions of the Northern Hemisphere (20°N-60°N), reflecting strong sampling biases and sparse observational coverage in the tropics and the Southern Hemisphere. This uneven coverage persists despite the high potential for elevated emissions in warm, frequently anoxic aquatic environments characteristic of these underrepresented regions (Flecker et al., 2022). Such geographic skewness is further reinforced by socioeconomic disparities in monitoring capacity and research investment. Over 80% of available measurements originate from high- and upper-middle-income economies, with China, contributing approximately 38%, and the United States, around 15%, dominating observed emission hotspots in intensively fertilized river basins such as the Yangtze and Mississippi rivers, respectively. In contrast, lower-income regions account for less than 6% of observations, restricting insights into large, comparatively understudied systems including the Congo and Amazon basins.

Additionally, clear urban biases are also evident in recorded datasets, predominantly for rivers and streams. Many high-emission records are derived from urbanized catchments, often from polluted rivers in China and Europe (Wang et al., 2022; Li et al., 2022), where aquatic bodies receive substantial inputs of treated wastewater effluents. For instance, rivers in rapidly urbanizing regions of East Asia exhibit N_2O fluxes that are significantly higher than those observed in natural forested or mountain catchments. Across economic contexts, observations from high-income countries such as the United States and

https://doi.org/10.5194/essd-2026-109
Preprint. Discussion started: 13 May 2026

Germany tend to cluster within agricultural-urban interfaces, with mean fluxes on the order of ~0.1-0.15 mmol m^{-2} d^{-1}. In contrast, hotspots in upper-middle-income economies, particularly China, frequently exceed 100 mmol m^{-2} d^{-1} in densely populated basins, indicating that population-driven river modification and nutrient loading can amplify N_2O emissions more strongly than in predominantly rural, low-income settings. Furthermore, the Southern Hemisphere remains notably underrepresented, especially at latitudes south of the equator, for both concentration and flux measurements, highlighting substantial knowledge gaps in high-latitude and southern tropical aquatic ecosystems (Kong et al., 2017; Zhu et al., 2025).

Although spatial coverage of N_2O measurements has improved considerably over the past decade, recent syntheses consistently highlight persistent limitations in temporal resolution. The majority of published datasets remain based on discrete sampling campaigns, often yielding only one or a small number of observations per site, which constrains the ability to capture short-term variability and episodic emission events (Cui et al., 2024; Que et al., 2023). In GANED, the temporal dimension of data availability reveals an exponential increase in observations since the early 2000s (Fig. 3c,d), reflecting growing scientific recognition of the role of aquatic bodies in the global N_2O budget.

4.3 Biogeochemical drivers and environmental controls

The primary objective of compiling GANED was to consolidate global N_2O data, providing a foundation for more comprehensive analyses in future research. To achieve this goal, the database integrates detailed observations that allow systematic exploration of the relationships between N_2O dynamics and potential environmental drivers. This integration facilitates a more robust evaluation of the factors controlling N_2O fluxes, and is expected to enhance the accuracy and reliability of assessments of N_2O distributions from regional to global scales, while improving quantification of aquatic emissions to the atmosphere. In this study, we examined a subset of key drivers, including NH_4^+, NO_3^-, NO_2^-, DO, DOC, TN, TP, water temperature, and salinity, for their correlations with N_2O flux records (Fig. 10). The inclusion of these drivers increases the utility of the dataset for comparative assessment and for evaluating patterns in relation to aquatic system type and sampling context. Correlation analyses in GANED identified that inorganic N species were the dominant positive drivers of N_2O emissions (NH_4^+: $R^2 = 0.943$, $p < 0.001$; NO_3^-: $R^2 = 0.691$, $p < 0.001$; NO_2^-: $R^2 = 0.807$, $p < 0.001$), whereas DO ($R^2 = -0.205$, $p = 0.048$) and water temperature ($R^2 = 0.07$, $p = 0.46$) exhibited negative or weak associations, highlighting denitrification as a key pathway (Xu et al., 2025). These strong correlations with inorganic N species further align with the understanding that N_2O is primarily produced as an intermediate or byproduct of microbial nitrification and denitrification processes (Amado and Roland, 2017). Further, moderate positive correlations with DOC suggest that carbon availability enhances heterotrophic processes, with lower DOC:NO_3^- ratios (carbon-limited conditions) likely promoting incomplete denitrification and N_2O production, whereas high DOC: NO_3^- ratios (carbon-rich conditions) may favor DNRA or assimilation in nutrient-enriched systems. The relationship between TP and N_2O was non-significant and exhibited substantial data variability, suggesting that TP exerts minimal direct control over N_2O dynamics. Although, TP is a well-documented driver of eutrophication (Dodds and Smith, 2016), its potential indirect influence on N_2O production through algal bloom warrants further investigation (Wang et al., 2023). Additionally, the observed correlation between DO and N_2O flux indicate that oxygen availability partially regulates

https://doi.org/10.5194/essd-2026-109
Preprint. Discussion started: 13 May 2026

N_2O production, with hypoxic conditions in warmer waters promoting high N_2O production. This pattern is consistent with observations from oxygen-deficient zones, which are estimated to contribute over half of global oceanic N_2O emissions (Wang et al., 2025).

Environmental drivers of N_2O fluxes vary across aquatic system types, reflecting distinct biogeochemical mechanisms. Within GANED, rivers and streams (176 of 436 study sources) exhibit high NH_4^+ and NO_3^- concentrations derived from runoff and sewage inputs, which drive nitrification in oxic zones and incomplete denitrification in hypoxic reaches, further intensified by flow turbulence. Moreover, urban river showed amplified fluxes under low DO conditions. Lakes and reservoirs (94 sources) which are characterized by high mean nutrient concentrations, experience stratification that induces hypolimnetic anoxia, exacerbating denitrification. Reservoirs, in particular, exhibit pulsed N_2O emissions modulated by temperature and nutrient gradients (Leon-Palmero et al., 2025). Estuaries (57 sources), despite lower means fluxes, exhibit strong influences of salinity ($R^2 = 0.636$, $p = 0.005$) and hydrodynamic mixing, which promote coupled nitrification-denitrification at interfaces (Maxey et al., 2024), with nutrient pulses from upstream further increasing variability. Ponds and aquaculture (40 sources; intermediate fluxes) are affected by intensive management practices that elevate NH_4^+ loading and stimulate nitrification, while anoxic sediments drive denitrification (Wang et al., 2023), though aeration can suppress N_2O production. In seas and coastal areas, dilution and equilibrium generally suppress fluxes, although upwelling zones with low DO can create localized N_2O hotspots via denitrification (Lachkar et al., 2024). Across this GANED database's diverse aquatic types, nutrient inputs emerge as a universal driver of emissions, with urban pollution amplifying fluxes in inland waters. In contrast, less-impacted natural waters are primarily sensitive to DO and DOC (Yoon et al., 2023), highlighting the interplay between nutrient availability and redox conditions in regulating N_2O production.

Furthermore, a ML approach using the RF model revealed that inorganic N substrates, particularly NO_3^- and NH_4^+, consistently rank among the top predictors of N_2O fluxes in freshwater and estuarine waters (Fig. 11), supporting substrate availability as a primary global driver (Liu et al., 2025). Collectively, these N species account for nearly 40% of total predictive importance. In addition, other environmental drivers, including DO, water temperature, and salinity, exert stronger influence in specific aquatic types, reflecting the heterogeneity of N_2O emission mechanisms. Among these, the weak correlation between water temperature and N_2O flux conceals pronounced system-specific variability. Temperature exerts divergent effects across aquatic systems, depending on the dominant N_2O production pathways, substrate availability, and physical structure. In stratified systems, such as lakes and reservoirs, temperature primarily influences N_2O emissions indirectly by promoting thermal stratification, which induces hypolimnetic anoxia and decouples zones of N_2O production from surface emission interfaces (Li et al., 2024; Wu et al., 2024). In contrast, in well-mixed shallow systems, including rivers, streams, and shallow ponds, temperature directly stimulates microbial metabolic activity associated with both nitrification and denitrification, resulting in a positive relationship between temperature and N_2O emissions (Wang et al., 2023). Moreover, DO emerges as a critical secondary regulator (Fig. 10), reflecting the sensitivity of N_2O production to redox conditions, whereas salinity plays a relatively minor role at the global scale (Li et al., 2019). The rankings of these predictors align with the central role of nitrification and denitrification as the dominant microbial pathways of N_2O production in aquatic environments (Yao et al.,

https://doi.org/10.5194/essd-2026-109
Preprint. Discussion started: 13 May 2026

2020; Kuypers et al., 2018). The pronounced importance of NO_3^- reflects its function as the terminal electron acceptor in denitrification and its accumulation under oxic and sub-oxic conditions, which favor incomplete reduction to N_2O rather than N_2 (Benckiser et al., 2015; Hassan et al., 2022). Similarly, high NH_4^+ feature importance indicates substantial contribution from nitrifier denitrification and hydroxylamine oxidation, processes that dominate in environments with elevated NH_4^+ loading (Zhang et al., 2023). Importantly, these outcomes are derived directly from empirical patterns within GANED rather than from model assumptions or literature-derived interpretation, providing an evidence-based foundation for targeted future process studies.

4.4 Dataset heterogeneity and implications for interpretation

A notable feature of GANED is the strong heterogeneity in reported N_2O concentrations and fluxes across sites, aquatic types, and observation methods. This heterogeneity reflects both natural environmental variation and differences in sampling design, observation frequency, and measurement approach across the source literature. Rather than attempting to remove this variability, the database preserves it in a harmonized structure so that users can evaluate patterns, filter records, and define subsets appropriate to their applications. The skewed distributions within GANED, illustrated by approximately 13% of zero or negative fluxes, combined with pronounced spatial heterogeneity, including Northern Hemisphere and economic biases, indicate that current global N_2O estimates likely remain incompletely represented, which should be acknowledged in broad-scale interpretations derived from the database. Although the sparse data from these regions suggest lower peak fluxes, they may nonetheless harbor significant emission hotspots under warming scenarios. This heterogeneity observed in GANED should be regarded as an inherent characteristic of global aquatic N_2O observations, rather than a limitation of the database.

Consistent with the patterns discussed in Sect. 4.1-4.3, this variability reflects real differences in the processes governing N_2O production and emission across diverse aquatic system types and environmental contexts. Rivers and streams, which account for roughly 80% of high-emission records, highlight the potential for targeted mitigation strategies, such as riparian buffer implementation, to reduce denitrification-driven N_2O production (Slate et al., 2024; Wang et al., 2025).

In contrast, lakes and reservoirs exhibit broader but more episodic variability, pointing to a dominant role of internally regulated processes. Here, stratification and the transient accumulation of reactive N can trigger short-lived emission peaks rather than persistently elevated fluxes (Shen et al., 2025**)**. Estuaries represent intermediate emissions, where the interplay between freshwater and marine inputs, along with organic-rich sediments, modulates the balance between N_2O production and consumption. This dynamic is evident in our RF-model analyses, which identify salinity, DO, and NO_3^- as key predictors in these systems (Fig. 11 and Fig. S2). Seas and coastal waters exhibit comparatively low median N_2O fluxes in the current dataset; however, the broad variability and limited sampling of oxygen-deficient or eutrophic boundary zones suggest that these patterns likely reflect observational gaps rather than consistently low emissions.

Overall, the heterogeneity observed in GANED is structured and interpretable. It illustrates how key drivers identified in this study, particularly inorganic N availability and redox conditions, manifest differently across hydrological contexts, providing an empirical foundation for assessing the ability of models to reproduce these cross-system contrasts in N_2O emission dynamics.

https://doi.org/10.5194/essd-2026-109
Preprint. Discussion started: 13 May 2026

Furthermore, comparisons with concurrent GHG datasets (CO_2 and CH_4; Table S1; Fig. S1) reveal co-emission patterns, supporting the development of integrated aquatic GHG budgets, in which N_2O accounts for roughly 7-10% of total aquatic emissions.

4.5 Limitations, gaps, and future data needs

Despite broad coverage, GANED inherits several limitations from its underlying observational sources. Some aquatic environments such as intermittent or transitional systems remain weakly represented, and some pathways or ancillary variables are insufficiently documented in the available literature. The datasets exhibit pronounced spatial biases, with approximately 60% of sites located in Asia and an additional 15% in North America. This imbalance highlights the need for expanded monitoring in underrepresented regions to reduce uncertainties in global flux estimates. Long-term records were scarce in the dataset, with only 2-4% of sites having more than 10 observations, limiting the ability to resolve interannual trends. Similarly, the scarcity of long-term time series (>10 years) at most sites limits our ability to discern climate-driven trends, interannual variability, and the effects of extreme events on N_2O emissions. Currently, no continuous records exist for N_2O fluxes, and most available concentration data are limited to a small number of geographically clustered sites.

Furthermore, investigations in arid drainage systems remain particularly limited, more so than anticipated based on their relatively small river surface area. This specific gap likely reflects the dominant research focus on streams and rivers as major, continuous contributors to the global atmospheric N_2O budget (Tikkasalo et al., 2025), leading to the assumption that arid systems contribute relatively little. In such systems, dry-wet alternations and transient inundation events can substantially influence N_2O dynamics by shifting redox conditions, altering nutrient availability, and stimulating microbial processes (De Klein et al., 2017). For instance, ephemeral streams, floodplains, and reservoirs in arid and semi-arid regions may remain inactive during dry phases but emit significant N_2O pulses upon rewetting (Webb et al., 2023; Stringer et al., 2021). Thus, what may initially appear as a "gap from arid zones" is more accurately a lack of representation of intermittent and transitional aquatic systems, which likely contribute disproportionately to regional N_2O budgets (Upadhyay et al., 2023). One of the most persistent gaps in current flux data collection is the limited quantification of plant-mediated emissions. Although such fluxes can account for a substantial proportion of total N_2O release in wetlands and shallow lakes (Bodmer et al., 2021), their contribution to other aquatic systems remains largely unquantified. In our GANED database, plant-mediated fluxes were excluded, as only two studies were found to explicitly report this pathway in streams (Sanders et al., 2007; Wilcock and Sorrell, 2008). These limitations identify priorities for future data collection and database expansion rather than shortcomings unique to GANED itself.

Future efforts should prioritize the development of automated sampling technologies, such as field-deployable online GHG monitoring systems for dissolved N_2O (Piatka et al., 2024), to improve temporal resolution and reduce observational gaps. Integrating these high-frequency measurements with machine-learning approaches will further enhance gap-filling and support predictive modeling across diverse aquatic systems. Additionally, coupling in situ observations with remote-sensing products and global hydrological models will enable more robust upscaling of flux estimates and help narrow uncertainties in the global

https://doi.org/10.5194/essd-2026-109
Preprint. Discussion started: 13 May 2026

aquatic N_2O budget. By making GANED openly accessible, we aim to facilitate continuous community-driven updates that strengthen flux estimates and support forthcoming IPCC AR7 assessments (IPCC, 2023). Collectively, these advances will help inform targeted mitigation strategies, ranging from wetland restoration to precision nutrient management, to reduce aquatic N_2O emissions and contribute to achieving the 1.5 °C climate targets.

5 Code and data availability

The scripts used for data harmonization, quality-control processing, statistical analysis, and figure generation are archived in Environmental Data Initiative (EDI) and are available at: https://doi.org/10.6073/pasta/4a086e49a4f308679b951293b380e7b9 (Nazir et al., 2026). The archived materials include the R scripts used for unit conversion, data cleaning, statistical summaries, Random Forest analysis, and manuscript figure production. Dataset sheets and code archives are documented in repository (edi.2267.1) to support reproducibility.

6 Conclusion

The Global Aquatic N_2O Emission Database (GANED) represents the most comprehensive synthesis of empirical N_2O observations, encompassing 5,130 dissolved concentration records and 7,386 flux measurements from diverse aquatic types, including rivers, streams, lakes, reservoirs, ponds, estuaries, seas, and coastal areas, spanning 1980-2023. By harmonizing data from 426 peer-reviewed sources and explicitly linking N_2O dynamics to co-measured biogeochemical drivers, GANED reveals pronounced heterogeneity in emission patterns across aquatic bodies. GANED improves access to previously fragmented information and supports more transparent comparison across aquatic system types. Rivers and streams emerge as dominant emission hotspots, exhibiting the highest and most variable fluxes, primarily driven by elevated inorganic N substrates, such as NH_4^+, NO_3^-, and NO_2^-. In contrast, lakes, reservoirs, estuaries, and ponds show intermediate levels, and open seas and coastal waters consistently display lower emissions, occasionally functioning as weak N_2O sinks. Random forest analyses further confirm substrate availability as the primary global control on aquatic N_2O production, with redox conditions such as DO exerting secondary but system-specific influences. These patterns highlight the central role of microbial nitrification, denitrification, and nitrifier-denitrification pathways in regulating aquatic N_2O emissions.

GANED advances N_2O research by providing the first global dataset that systematically distinguishes emission mechanisms across aquatic system types through interlinked biogeochemical metadata. Critically, it demonstrates that aquatic N_2O emissions are primarily substrate-controlled rather than climate-controlled, and reveals systematic biases from concentration-only measurements that may underestimate fluxes in dynamic systems like streams. Despite substantial progress in observational coverage since 2000, GANED highlights persistent spatial biases, such as concentrated observations (~60% of sites) in Asia, and critical data gaps in Africa, South America, high-latitude regions, and low-income economies. These economic disparities result in well-documented emissions in high-income countries (China, the United States) while substantial

https://doi.org/10.5194/essd-2026-109
Preprint. Discussion started: 13 May 2026

gaps persist in low- and middle-income regions. These imbalances, together with the scarcity of long-term time series and the underrepresentation of intermittently connected or episodic systems, likely contribute to considerable uncertainty in current global aquatic N_2O budgets. Existing estimates suggest that inland waters, estuaries, and oceans together account for approximately 25-32% (≈ 5.3 Tg N yr^{-1}) of total anthropogenic N_2O emissions, yet the pronounced economic and latitudinal skew in GANED implies that contributions from tropical and Southern Hemisphere systems may be systematically underestimated.

GANED marks a pivotal shift from documenting "where" emissions occur to understanding "why" they differ across systems, enabling targeted mitigation interventions. Moreover, GANED provides an essential empirical foundation for refining national GHG inventories, improving process-based and machine-learning models, and identifying targeted mitigation opportunities. By elucidating mechanistic rather than purely spatial controls on emissions, the database shifts the paradigm from treating aquatic systems as uniform "hotspots" toward recognizing substrate-driven heterogeneity amenable to management. In particular, the results highlight the potential effectiveness of reducing N loading in rivers, streams, and urban-impacted waters. Making GANED reusable synthesis product for comparative analysis, intercomparison, and future refinement of aquatic N_2O assessments will facilitate community-driven expansion, integration with emerging high-frequency and remote-sensing products, and more robust constraints on aquatic N_2O contributions in future IPCC assessments.

https://doi.org/10.5194/essd-2026-109
Preprint. Discussion started: 13 May 2026

7 Appendices

Appendix A: GANED tables and variables

Table A1: Column titles and description of their content for the GANED "Data Source" component.

Column title	Description
Title	Title of data source
Author	Last name of the leading author.
Type	Type of data source either its Journal article, master's thesis or doctoral dissertation
SRC-Name	Name of the data source outlet, such as a journal, data repository. For studies with both published papers and associated datasets, the journal name is listed here.
Pub-year	Year of publication, data release, or acquisition of an unpublished dataset.
Source-ID	Unique identifier assigned to the data source.
Paper-DOI	DOI or hyperlink for the journal article or other publication reporting the N_2O data.
Additional-data	"Marked "Yes" if additional data were obtained directly from the author for any field.

https://doi.org/10.5194/essd-2026-109
Preprint. Discussion started: 13 May 2026

Table A2: Column titles and content description for the GANED "Sampling Sites".

Column title	Definition
Source-ID	Unique identifier assigned to each data source in the 'Data Source' dataset.
Site-ID	Unique identifier for each sampling site.
Continent	Asia, Africa, North America, South America, Antarctica, Europe, Australia
Country	Countries categorized by their continents/sub-continents
Aquatic-type	Water bodies based on their ecological characteristics (lakes, rivers, ponds, estuary, reservoirs, coastal area, sea)
Site-Name	Name assigned to the site.
Region-Name	Name of the area from the data source taken based on the specified region.
Latitude	Geographic latitude (decimal degrees) in the WGS84 ensemble (EPSG:4326).
Longitude	Geographic longitude (decimal degrees) in the WGS84 ensemble (EPSG:4326).
Elevation-m	Reported elevation of the site (meters above sea level).
Slope-m-per-m	Reported channel slope (m m^{-1}).
Status	N_2O Concentration, flux or records containing both
Channel-type	Codes describing specific channel attributes or site conditions; categories and definitions are provided in Table 1.
Comments	Additional information or clarifications regarding the site or data source (if any).

https://doi.org/10.5194/essd-2026-109
Preprint. Discussion started: 13 May 2026

Open Access Earth System Science Data Discussions

775 **Table A3: Column titles and definitions for the GANED "Concentration dataset".**

Column title	Definition
Source-ID	Unique identifier for each publication in the 'Data Source' component.
Site-ID	Unique identifier for each sampling site in the 'Sampling Sites'.
Site-Name	Unique name of the sampling site from the "Sites" component.
Conc-Name	Identifier for the sampling event at a site. Matches Conc-Name when concentration measurements exist for the same site-date combination.
Sampling-year	Corresponding year of observation recorded.
Sampling-month	Monthly precision of observation data of targeted site.
Date-start	First date of sample collection.
Date-end	Last date of sample collection; identical to Date-start if data are not aggregated over time.
Aggregated-Space	Indicates whether values are averaged across more than one site ("yes" or "no").
Aggregated-Time	Indicates whether values are averaged across more than one sampling date ("yes" or "no").
Observation type	sources providing only gas concentration marked as 'Conc' and for Conc+flux marked as 'Both'.
N_2O concentration	Concentration records of N_2O (μmol L^{-1}) from sampling sites.
CO_2 concentration	CO_2 concentration (μmol L^{-1}) measured concurrently with N_2O.
CH_4 Concentration	CH_4 concentration (μmol L^{-1}) measured concurrently with N_2O.

https://doi.org/10.5194/essd-2026-109
Preprint. Discussion started: 13 May 2026

Open Access Earth System Science Data Discussions

Table A4: Column titles and definitions for the GANED "Flux dataset".

Column Title	Definition
Source-ID	Unique paper identifier from the data source
Site-ID	Unique site identifier from the sampling sites
Site-Name	Unique site name from the sampling sites
Flux-Name	Unique name for the sampling event at the site; same as Conc-Name in the concentration table if both concentration and flux data for the same site-date combination are available
Date-start	First sampling date
Date-end	Last sampling date; this is the same date as Date-start if data are not aggregated over time.
Aggregated-Space	Yes or no; "yes" if N_2O data entered are averages from >1 site
Aggregated-Time	Yes or no; "yes" if N_2O data entered are averages from >1 date
Flux-Method	Methodological category used to measure diffusive gas flux. Categories (with brief explanations in italics) are the following. – *chamber (unspecified) – unspecified response* use of an unspecified type of chamber (static or free-floating) and pattern of change gas concentration – *floating chamber – unspecified response* chamber unrestrained and able to float downstream during flux measurement – *floating chamber – linear response* – *conc+k* diffusive flux calculated using the equation flux= k (Cw - Ceq), where k is gas exchange coefficient, Cw=N_2O concentration measured in water, and Ceq=N_2O concentration in water in equilibrium with the atmosphere
N_2O-Flux	Total measured N_2O flux (mmolm^2 d^{-1})
CO_2_Flux	measured total CO_2 flux (mmolm^2 d^{-1})
CH_4-Flux	measured total CH_4 flux (mmolm^2 d^{-1})
Total-N_2O-Flux-SD	Standard deviation of the mean total N_2O flux
Total_N_2O_Flux_Median	Median measured total N_2O flux (mmolm^2 d^{-1})
Comments	Any additional relevant information regarding data entered in this row
Flux-unit	Common unit for all diffusive N_2O flux data (mmol m^{-2} day^{-1})
DO-mgL	Dissolved oxygen (mg L^{-1}).
pH	pH of the water sample.
NO_3	Nitrate or nitrite + nitrate concentration (µmol L^{-1}) measured concurrently with N_2O.
NH_4	Ammonium concentration (µmol L^{-1}) measured concurrently with N_2O.
TN	Total nitrogen (TN) measured concurrently with N_2O.
TP	Total phosphorus (TP) measured concurrently with N_2O.
DOC	Dissolved organic carbon (DOC) measured concurrently with N_2O.
WaterTemp-degC	Water temperature (_C) measured concurrently with N_2O.

https://doi.org/10.5194/essd-2026-109
Preprint. Discussion started: 13 May 2026

8 Supplement.

The supplement related to this article is available online at: https://doi.org/XXXXX/essd.-supplement.

9 Author Contribution

Muhammad Junaid Nazir and Longfei Yu conceptualized the study and writing the original draft. Jing Wei investigated, supervised and review the study. Yunjie Zhang, Jing Zou and Wenping Yuan conducted the analysis, data curation and prepared figures. All authors contributed to the investigation, visualization, data acquisition, data entry, data checking, writing, reviewing and editing the original draft.

10 Competing interests

The authors declare that they have no conflict of interest.

11 Acknowledgements

We are grateful to all the authors who generously shared data or made their data public; our science is better for this transparency. We are also grateful to several of these investigators for patiently and thoughtfully responding to emails for data curation and additional information required. We also thank anonymous reviewers for useful discussions and feedback on earlier versions of this manuscript. We are grateful to all authors for providing essential data, and to Software Developers for tools that facilitated our analysis.

12 Financial Support

This work was financially supported by the Guangdong Basic and Applied Basic Research Foundation (2025B1515020013, 2025A1515012987), the Science and Technology Program of Guangdong (2024B1212070012), National Natural Science Foundation of China (42577331，42271269），National Key Research and Development Program the National Natural Science Foundation of China (2023YFF0805403), Basic Scientific Research Operating Expenses of Central Universities (C24wkjc14), and the Scientific Research Start-up Funds (QD2022010C) from Tsinghua Shenzhen International Graduate School.

https://doi.org/10.5194/essd-2026-109
Preprint. Discussion started: 13 May 2026

13 References

Amado, A. M. and Roland, F.: Microbial role in the carbon cycle in tropical inland aquatic ecosystems, https://doi.org/10.3389/978-2-88945-127-2, 2017.

Ansari, J., Bardhan, S., Davis, M. P., Anderson, S. H., and Al-Awwal, N.: Greenhouse gas emissions from riparian systems as affected by hydrological extremes: a mini-review, Cogent Food & Agriculture, 10, 2321658, https://doi.org/10.1080/23311932.2024.2321658, 2024.

Benckiser, G., Schartel, T., and Weiske, A.: Control of NO_3^- and N_2O emissions in agroecosystems: a review, Agronomy for sustainable development, 35, 1059-1074, https://doi.org/10.1007/s13593-015-0296-z, 2015.

Bodmer, P., Vroom, R., Stepina, T., del Giorgio, P. A., and Kosten, S.: Methane fluxes of vegetated areas in natural freshwater ecosystems: assessments and global significance, https://doi.org/10.31223/X5ND0F, 2021.

Butler, J. H. Z.: Cycling of reduced trace gases and hydroxylamine in coastal waters, PhD Dissertation, Oregon State University, 1986.

Call, M., Sanders, C. J., Enrich-Prast, A., Sanders, L., Marotta, H., Santos, I. R., and Maher, D. T.: Radon-traced pore-water as a potential source of CO_2 and CH_4 to receding black and clear water environments in the Amazon Basin, Limnology and Oceanography Letters, 3, 375-383, https://doi.org/10.1002/lol2.10089, 2018.

Christensen, S. and Rousk, K.: Global N_2O emissions from our planet: Which fluxes are affected by man, and can we reduce these?, iScience, 27, 109042, https://doi.org/10.1016/j.isci.2024.109042, 2024.

Crawford, J. T. and Stanley, E. H.: Controls on methane concentrations and fluxes in streams draining human-dominated landscapes, Ecological Applications, 26, 1581-1591, https://doi.org/10.1890/15-133, 2016.

Cui, P., Cui, L., Zheng, Y., and Su, F.: Land use and urbanization indirectly control riverine CH_4 and CO_2 emissions by altering nutrient input, Water Research, 265, 122266, https://doi.org/10.1016/j.watres.2024.122266, 2024.

Davidson, E. A. and Kanter, D.: Inventories and scenarios of nitrous oxide emissions, Environmental Research Letters, 9, 105012, https://doi.org/10.1088/1748-9326/9/10/105012, 2014.

De Klein, J. J., Overbeek, C. C., Juncher Jørgensen, C., and Veraart, A. J.: Effect of temperature on oxygen profiles and denitrification rates in freshwater sediments, Wetlands, 37, 975-983, https://doi.org/10.1007/s13157-017-0933-1, 2017.

De la Paz, M., Velo, A., Steinfeldt, R., and Pérez, F. F.: The unaccounted oceanic sink of anthropogenic nitrous oxide and its relationship with anthropogenic carbon dioxide, Global biogeochemical cycles, 39, e2024GB008417, https://doi.org/10.1029/2024GB008417, 2025.

De Wilde, H. P. J. and de Bie, M. J. M.: Nitrous oxide in the Schelde estuary: production by nitrification and emission to the atmosphere, Marine Chemistry, 69, 203-216, https://doi.org/10.1016/S0304-4203(99)00106-1, 2000.

Dodds, W. K. and Smith, V. H.: Nitrogen, phosphorus, and eutrophication in streams, Inland Waters, 6, 155-164, https://doi.org/10.5268/IW-6.2.909, 2016.

Dowle, M. and Srinivasan, A.: data. table: extension of 'data. frame'. R package version 1.14. 2. 2021,

https://doi.org/10.5194/essd-2026-109
Preprint. Discussion started: 13 May 2026

https://doi.org/10.32614/CRAN.package.data.table, 2023.

Duvert, C., Borges, A. V., Calamita, E., Rocher-Ros, G., Linkhorst, A., Rosentreter, J. A., Liu, S., Taillardat, P., Attermeyer, K., and DelSontro, T.: Hydroclimate and landscape diversity drive highly variable greenhouse gas emissions from tropical and subtropical inland waters, Nature Water, 1-15, https://doi.org/10.1038/s44221-025-00522-8, 2025.

Flecker, A. S., Shi, Q., Almeida, R. M., Angarita, H., Gomes-Selman, J. M., García-Villacorta, R., Sethi, S. A., Thomas, S. A., Poff, N. L., and Forsberg, B. R.: Reducing adverse impacts of Amazon hydropower expansion, Science, 375, 753-760, https://doi.org/10.1126/science.abj4017, 2022.

Gong, C., Tian, H., Liao, H., Pan, N., Pan, S., Ito, A., Jain, A. K., Kou-Giesbrecht, S., Joos, F., and Sun, Q.: Global net climate effects of anthropogenic reactive nitrogen, Nature, 632, 557-563, https://doi.org/10.1038/s41586-024-07714-4, 2024.

Hall Jr, R. O. and Ulseth, A. J.: Gas exchange in streams and rivers, Wiley Interdisciplinary Reviews: Water, 7, e1391, https://doi.org/10.1002/wat2.1391, 2020.

Hassan, M. U., Aamer, M., Mahmood, A., Awan, M. I., Barbanti, L., Seleiman, M. F., Bakhsh, G., Alkharabsheh, H. M., Babur, E., and Shao, J.: Management strategies to mitigate N_2O emissions in agriculture, Life, 12, 439, https://doi.org/10.3390/life12030439, 2022.

He, C., Qi, R., Feng, H., Zhao, Z., Wang, F., Wang, D., Wang, F., Chen, X., Zhang, P., and Li, S.: Spatiotemporal variations and dominated environmental parameters of nitrous oxide (N_2O) concentrations from cascade reservoirs in southwest China, Environmental Science and Pollution Research, 30, 102547-102559, https://doi.org/10.1007/s11356-023-29502-9, 2023.

He, G., Chen, G., Xie, Y., Swift, C. M., Ramirez, D., Cha, G., Konstantinidis, K. T., Radosevich, M., and Löffler, F. E.: Sustained bacterial N_2O reduction at acidic pH, Nature Communications, 15, 4092, https://doi.org/10.1038/s41467-024-48236-x, 2024.

Hu, M., Chen, D., and Dahlgren, R. A.: Modeling nitrous oxide emission from rivers: a global assessment, Global change biology, 22, 3566-3582, https://doi.org/10.1111/gcb.13351, 2016.

Intergovernmental Panel on Climate, C.: Climate Change 2021 – The Physical Science Basis: Working Group I Contribution to the Sixth Assessment Report of the Intergovernmental Panel on Climate Change, Cambridge University Press, Cambridge, https://doi.org/10.1017/9781009157896, 2023.

Intergovernmental Panel on Climate, C.: Global Warming of 1.5°C: IPCC Special Report on Impacts of Global Warming of 1.5°C above Pre-industrial Levels in Context of Strengthening Response to Climate Change, Sustainable Development, and Efforts to Eradicate Poverty, Cambridge University Press, Cambridge, https://doi.org/10.1017/9781009157940, 2022.

Kabacoff, R.: Modern data visualization with R, Chapman and Hall/CRC, https://doi.org/10.1201/9781003299271, 2024.

Kong, D., Zhang, Q., Singh, V. P., and Shi, P.: Seasonal vegetation response to climate change in the Northern Hemisphere (1982-2013), Global and Planetary Change, 148, 1-8, https://doi.org/10.1016/j.gloplacha.2016.10.020, 2017.

Kuypers, M. M., Marchant, H. K., and Kartal, B.: The microbial nitrogen-cycling network, Nature Reviews Microbiology, 16, 263-276, https://doi.org/10.1038/nrmicro.2018.9, 2018.

https://doi.org/10.5194/essd-2026-109
Preprint. Discussion started: 13 May 2026

Lachkar, Z., Cornejo-D'Ottone, M., Singh, A., Arístegui, J., Dewitte, B., Fawcett, S., Garçon, V., Lovecchio, E., Molina, V., and Vinayachandran, P.: Biogeochemistry of greenhouse gases in coastal upwelling systems: Processes and sensitivity to global change, Elem Sci Anth, 12, 00088, https://doi.org/10.1525/elementa.2023.00088, 2024.

Lauerwald, R., Bastos, A., McGrath, M. J., Petrescu, A. M. R., Ritter, F., Andrew, R. M., Berchet, A., Broquet, G., Brunner, D., and Chevallier, F.: Carbon and greenhouse gas budgets of Europe: Trends, interannual and spatial variability, and their drivers, Global Biogeochemical Cycles, 38, e2024GB008141, https://doi.org/10.1029/2024GB008141, 2024.

Lauerwald, R., Bastviken, D., Battin, T., Ciais, P., Tian, H., Allen, G., Abril, G., Catalan, N., Deemer, B., and del Giorgio, P.: Global Inland Water Greenhouse Gas Emissions: Patterns, Trends, and Anthropogenic Drivers, https://doi.org/10.5194/egusphere-egu25-13764, 2025.

Lehner, B., Anand, M., Fluet-Chouinard, E., Tan, F., Aires, F., Allen, G. H., Bousquet, P., Canadell, J. G., Davidson, N., and Finlayson, C. M.: Mapping the world's inland surface waters: an update to the Global Lakes and Wetlands Database (GLWD v2), Earth System Science Data Discussions, 2024, 1-49, https://doi.org/10.5194/essd-2024-204, 2024.

Lemon, E. and Lemon, D.: Nitrous oxide in fresh waters of the Great Lakes Basin, Limnology and Oceanography, 26, 867-879, https://doi.org/10.4319/lo.1981.26.5.0867, 1981.

Leon-Palmero, E., Morales-Baquero, R., and Reche, I.: Higher emissions of carbon dioxide, nitrous oxide, and methane during the daytime in two reservoirs, Biogeochemistry, 168, 99, https://doi.org/10.1007/s10533-025-01283-y, 2025.

Li, X., Gao, D., Hou, L., and Liu, M.: Salinity stress changed the biogeochemical controls on CH_4 and N_2O emissions of estuarine and intertidal sediments, Science of The Total Environment, 652, 593-601, https://doi.org/10.1016/j.scitotenv.2018.10.294, 2019.

Li, X., Yu, Y., Fan, H., and Tang, C.: Intense denitrification and sewage effluent result in enriched ^{15}N in N_2O from urban polluted rivers, Journal of Hydrology, 608, 127631, https://doi.org/10.1016/j.jhydrol.2022.127631, 2022.

Li, Y., Tian, H., Yao, Y., Shi, H., Bian, Z., Shi, Y., Wang, S., Maavara, T., Lauerwald, R., and Pan, S.: Increased nitrous oxide emissions from global lakes and reservoirs since the pre-industrial era, Nature Communications, 15, 942, https://doi.org/10.1038/s41467-024-45061-0, 2024.

Liang, J., Tang, W., Zhu, Z., Li, S., Wang, K., Gao, X., Li, X., Tang, N., Lu, L., and Li, X.: Spatiotemporal variability and controlling factors of indirect N_2O emission in a typical complex watershed, Water Research, 229, https://doi.org/10.1016/j.watres.2022.119515, 2023.

Liu, J., Zhang, Y., Jiang, S., Xiong, Y., Jin, C., Yu, Q., and Ma, W.: Atmospheric nitrogen deposition fluxes into coastal wetlands and their impacts on ecosystem carbon sequestration in East Asia, EGUsphere, 2025, 1-18, https://doi.org/10.5194/egusphere-2025-3801, 2025.

Lu, C., Zhang, J., Yi, B., Calderon, I., Feng, H., Miao, R., Hennessy, D., Pan, S., and Tian, H.: Riverine nitrogen footprint of agriculture in the Mississippi-Atchafalaya River Basin: do we trade water quality for crop production?, Environmental Research Letters, 18, 114043, https://doi.org/10.1088/1748-9326/ad0128, 2023.

Marzadri, A., Amatulli, G., Tonina, D., Bellin, A., Shen, L. Q., Allen, G. H., and Raymond, P. A.: Global riverine nitrous oxide

https://doi.org/10.5194/essd-2026-109
Preprint. Discussion started: 13 May 2026

emissions: The role of small streams and large rivers, Science of The Total Environment, 776, 145148, https://doi.org/10.1016/j.scitotenv.2021.145148, 2021.

Masson-Delmotte, V.: The physical science basis of climate change empowering transformations, insights from the IPCC AR6 for a climate research agenda grounded in ethics, PLOS Climate, 3, e0000451, https://doi.org/10.1371/journal.pclm.0000451, 2024.

Maxey, J. D., Hartstein, N. D., Bange, H. W., and Müller, M.: Nitrous oxide (N_2O) in Macquarie Harbour, Tasmania, Biogeosciences, 21, 5613-5637, https://doi.org/10.5194/bg-21-5613-2024, 2024.

Mishra, A., Singh, I., and Srinivasan, A.: Data Handling and Manipulation in R with Descriptive Statistics, in: R for Basic Biostatistics in Medical Research, Springer, 29-62, https://doi.org/10.1007/978-981-97-6980-3_4, 2024.

Moher, D., Liberati, A., Tetzlaff, J., Altman, D. G., Antes, G., Atkins, D., Barbour, V., Barrowman, N., Berlin, J., and Clark, J.: Preferred reporting items for systematic reviews and meta-analyses: the PRISMA statement, Revista Espanola de Nutricion Humana y Dietetica, 18, 172-181, https://doi.org/10.14306/renhyd.18.3.114, 2014.

Nazir, M., L. Yu, Y. Zhang, J. Zou, W. Yuan, and J. Wei.: A Comprehensive Global Aquatic N_2O Emission Database (GANED): Unravelling N_2O Emission Patterns from Different Water Bodies, 1980-2023 ver 1, Environmental Data Initiative, https://doi.org/10.6073/pasta/4a086e49a4f308679b951293b380e7b9, 2026.

Pan, H., Zhou, Z., Zhang, S., Wang, F., and Wei, J.: N_2O emissions from aquatic ecosystems: a review, Atmosphere, 14, 1291, https://doi.org/10.3390/atmos14081291, 2023.

Piatka, D. R., Nánási, R. L., Mwanake, R. M., Engelsberger, F., Willibald, G., Neidl, F., and Kiese, R.: Precipitation fuels dissolved greenhouse gas (CO_2, CH_4, N_2O) dynamics in a peatland-dominated headwater stream: results from a continuous monitoring setup, Frontiers in Water, 5, 1321137, https://doi.org/10.3389/frwa.2023.1321137, 2024.

Priscu, J. C., Christner, B. C., Dore, J. E., Westley, M. B., Popp, B. N., Casciotti, K. L., and Lyons, W. B.: Supersaturated N_2O in a perennially ice-covered Antarctic lake: Molecular and stable isotopic evidence for a biogeochemical relict, Limnology and Oceanography, 53, 2439-2450, https://doi.org/10.4319/lo.2008.53.6.2439, 2008.

Qian, H., Yuan, Z., Chen, N., Zhu, X., Huang, S., Lu, C., Liu, K., Zhou, F., Smith, P., Tian, H., Xu, Q., Zou, J., Liu, S., Song, Z., Zhang, W., Wang, S., Liu, Z., Li, G., Shang, Z., Ding, Y., van Groenigen, K. J., and Jiang, Y.: Legacy effects cause systematic underestimation of N_2O emission factors, Nature Communications, 16, 2775, https://doi.org/10.1038/s41467-025-58090-0, 2025.

Que, Z., Wang, X., Liu, T., Wu, S., He, Y., Zhou, T., Yu, L., Qing, Z., Chen, H., and Yuan, X.: Watershed land use change indirectly dominated the spatial variations of CH_4 and N_2O emissions from two small suburban rivers, Journal of Hydrology, 619, 129357, https://doi.org/10.1016/j.jhydrol.2023.129357, 2023.

Ravishankara, A. R., Daniel, J. S., and Portmann, R. W.: Nitrous Oxide (N_2O): The Dominant Ozone-Depleting Substance Emitted in the 21st Century, Science, 326, 123-125, https://doi.org/10.1126/science.1176985, 2009.

Rees, A. P., Bange, H. W., Arévalo-Martínez, D. L., Artioli, Y., Ashby, D. M., Brown, I., Campen, H. I., Clark, D. R., Kitidis, V., and Lessin, G.: Nitrous oxide and methane in a changing Arctic Ocean, Ambio, 51, 398-410,

https://doi.org/10.5194/essd-2026-109
Preprint. Discussion started: 13 May 2026

https://doi.org/10.1007/s13280-021-01633-8, 2022.

Resplandy, L., Hogikyan, A., Müller, J. D., Najjar, R. G., Bange, H. W., Bianchi, D., Weber, T., Cai, W. J., Doney, S. C., Fennel, K., Gehlen, M., Hauck, J., Lacroix, F., Landschützer, P., Le Quéré, C., Roobaert, A., Schwinger, J., Berthet, S., Bopp, L., Chau, T. T. T., Dai, M., Gruber, N., Ilyina, T., Kock, A., Manizza, M., Lachkar, Z., Laruelle, G. G., Liao, E., Lima, I. D., Nissen, C., Rödenbeck, C., Séférian, R., Toyama, K., Tsujino, H., and Regnier, P.: A Synthesis of Global Coastal Ocean Greenhouse Gas Fluxes, Global Biogeochemical Cycles, 38, https://doi.org/10.1029/2023GB007803, 2024.

Rosentreter, J. A., Wells, N. S., Ulseth, A. J., and Eyre, B. D.: Divergent gas transfer velocities of CO_2, CH_4, and N_2O over spatial and temporal gradients in a subtropical estuary, Journal of Geophysical Research: Biogeosciences, 126, e2021JG006270, https://doi.org/10.1029/2021JG006270, 2021.

Sanders, I., Heppell, C., Cotton, J., Wharton, G., Hildrew, A., Flowers, E., and Trimmer, M.: Emission of methane from chalk streams has potential implications for agricultural practices, Freshwater Biology, 52, 1176-1186, https://doi.org/10.1111/j.1365-2427.2007.01745.x, 2007.

Saunois, M., Stavert, A. R., Poulter, B., Bousquet, P., Canadell, J. G., Jackson, R. B., Raymond, P. A., Dlugokencky, E. J., Houweling, S., and Patra, P. K.: The global methane budget 2000–2017, Earth System Science Data Discussions, 2019, 1-136, https://doi.org/10.5194/essd-12-1561-2020, 2019.

Shen, W., Zhang, L., Ury, E. A., Li, S., Xia, B., and Basu, N. B.: Restoring small water bodies to improve lake and river water quality in China, Nature Communications, 16, 294, https://doi.org/10.1038/s41467-024-55714-9, 2025.

Silverthorn, T.: Greenhouse gas flux dynamics in fragmented river networks, Université Claude Bernard-Lyon I, https://theses.hal.science/tel-05128075v1, 2024.

Slate, M. L., Antoninka, A., Bailey, L., Berdugo, M. B., Callaghan, D. A., Cárdenas, M., Chmielewski, M. W., Fenton, N. J., Holland-Moritz, H., and Hopkins, S.: Impact of changing climate on bryophyte contributions to terrestrial water, carbon, and nitrogen cycles, New Phytologist, 242, 2411-2429, https://doi.org/10.1111/nph.19772, 2024.

Song, C., Liu, S., Wang, G., Zhang, L., Rosentreter, J. A., Zhao, G., Sun, X., Yao, Y., Mu, C., Sun, S., Hu, Z., Lin, S., Sun, J., Li, Y., Wang, Y., Li, Y., Raymond, P. A., and Karlsson, J.: Inland water greenhouse gas emissions offset the terrestrial carbon sink in the northern cryosphere, Sci Adv, 10, eadp0024, https://doi.org/10.1126/sciadv.adp0024, 2024.

Stanley, E. H., Loken, L. C., Casson, N. J., Oliver, S. K., Sponseller, R. A., Wallin, M. B., Zhang, L., and Rocher-Ros, G.: GRiMeDB: The global river database of methane concentrations and fluxes, Earth System Science Data Discussions, 2022, 1-94, https://doi.org/10.5194/essd-2022-346, 2022.

Stringer, L. C., Mirzabaev, A., Benjaminsen, T. A., Harris, R. M., Jafari, M., Lissner, T. K., Stevens, N., and Tirado-von Der Pahlen, C.: Climate change impacts on water security in global drylands, One Earth, 4, 851-864, https://doi.org/10.1016/j.oneear.2021.05.010, 2021.

Sun, W., Wang, D., Chen, Z., Hu, B., and Xu, S.: Concentrations and emission fluxes of CH_4 and N_2O in the river network of the Yangtze River Delta plain (in Chinese), Science China Press, 39, 165-175, https://doi.org/10.1007/s11426-009-0024-0, 2009.

https://doi.org/10.5194/essd-2026-109
Preprint. Discussion started: 13 May 2026

Team, R. C.: R Core Team R: a language and environment for statistical computing, Foundation for Statistical Computing, https://www.R-project.org/, 2025.

Thomer, A. K. and Rayburn, A. J.: "A patchwork of data systems": Quilting as an analytic lens and stabilizing practice for knowledge infrastructures, Science, Technology, & Human Values, 49, 1073-1102, https://doi.org/10.1177/01622439231175535, 2024.

Tian, H., Yang, J., Xu, R., Lu, C., Canadell, J. G., Davidson, E. A., Jackson, R. B., Arneth, A., Chang, J., and Ciais, P.: Global soil nitrous oxide emissions since the preindustrial era estimated by an ensemble of terrestrial biosphere models: Magnitude, attribution, and uncertainty, Global change biology, 25, 640-659, https://doi.org/10.1111/gcb.14514, 2019.

Tian, H., Xu, R., Canadell, J. G., Thompson, R. L., Winiwarter, W., Suntharalingam, P., Davidson, E. A., Ciais, P., Jackson, R. B., and Janssens-Maenhout, G.: A comprehensive quantification of global nitrous oxide sources and sinks, Nature, 586, 248-256, https://doi.org/10.1038/s41586-020-2780-0, 2020.

Tian, H., Pan, N., Thompson, R. L., Canadell, J. G., Suntharalingam, P., Regnier, P., Davidson, E. A., Prather, M., Ciais, P., and Muntean, M.: Global nitrous oxide budget (1980-2020), Earth System Science Data, 16, 2543-2604, https://doi.org/10.5194/essd-16-2543-2024, 2024.

Tikkasalo, O.-P., Peltola, O., Alekseychik, P., Heikkinen, J., Launiainen, S., Lehtonen, A., Li, Q., Martínez-García, E., Peltoniemi, M., and Salovaara, P.: Eddy-covariance fluxes of CO_2, CH_4 and N_2O in a drained peatland forest after clear-cutting, Biogeosciences, 22, 1277-1300, https://doi.org/10.5194/bg-22-1277-2025, 2025.

Tique, W. F. M., Sapena, M., Weigand, M., Groth, S., Geiß, C., and Taubenböck, H.: A comparative assessment of data-driven flood susceptibility mapping in Nigeria, https://doi.org/10.21203/rs.3.rs-6756403/v1, 2025.

Tonina, D., Marzadri, A., Bellin, A., Dee, M. M., Bernal, S., and Tank, J. L.: Nitrous oxide emissions from drying streams and rivers, Geophysical Research Letters, 48, e2021GL095305, https://doi.org/10.1029/2021GL095305, 2021.

Upadhyay, P., Prajapati, S. K., and Kumar, A.: Impacts of riverine pollution on greenhouse gas emissions: A comprehensive review, Ecological Indicators, 154, 110649, https://doi.org/10.1016/j.ecolind.2023.110649, 2023.

Van den Hoogen, J., Robmann, N., Routh, D., Lauber, T., van Tiel, N., Danylo, O., and Crowther, T. W.: A geospatial mapping pipeline for ecologists, BioRxiv, https://doi.org/10.1101/2021.07.07.451145, 2021.

Wang, G., Xia, X., Liu, S., Zhang, S., Yan, W., and McDowell, W. H.: Distinctive patterns and controls of nitrous oxide concentrations and fluxes from urban inland waters, Environmental Science & Technology, 55, 8422-8431, https://doi.org/10.1021/acs.est.1c00647, 2021a.

Wang, Y., Tian, Y., and Cao, Y.: Dam siting: a review, Water, 13, 2080, https://doi.org/10.3390/w13152080, 2021b.

Wang, X., Yu, L., Liu, T., He, Y., Wu, S., Chen, H., Yuan, X., Wang, J., Li, X., Li, H., Que, Z., Qing, Z., and Zhou, T.: Methane and nitrous oxide concentrations and fluxes from heavily polluted urban streams: Comprehensive influence of pollution and restoration, Environmental Pollution, 313, 120098, https://doi.org/10.1016/j.envpol.2022.120098, 2022.

Wang, J., Vilmin, L., Mogollón, J. M., Beusen, A. H. W., van Hoek, W. J., Liu, X., Pika, P. A., Middelburg, J. J., and Bouwman, A. F.: Inland Waters Increasingly Produce and Emit Nitrous Oxide, Environmental Science & Technology, 57, 13506-

https://doi.org/10.5194/essd-2026-109
Preprint. Discussion started: 13 May 2026

13519, https://doi.org/10.1021/acs.est.3c04230, 2023a.

Wang, Y., Peng, Y., Lv, C., Xu, X., Meng, H., Zhou, Y., Wang, G., and Lu, Y.: Quantitative discrimination of algae multi-impacts on N_2O emissions in eutrophic lakes: Implications for N_2O budgets and mitigation, Water Research, 235, 119857, https://doi.org/10.1016/j.watres.2023.119857, 2023b.

Wang, S., Huang, J., Wu, Z., Li, S., Zhu, X., Liu, Y., and Ji, G.: Global mapping of flux and microbial sources for oceanic N_2O, Nature Communications, 16, 3341, https://doi.org/10.1038/s41467-025-58715-4, 2025.

WATER, W. C.: WMO greenhouse gas bulletin, Sl: sn, https://gaw.kishou.go.jp/, 2019.

Webb, J. R., Quayle, W. C., Ballester, C., and Wells, N. S.: Semi-arid irrigation farm dams are a small source of greenhouse gas emissions, Biogeochemistry, 166, 123-138, https://doi.org/10.1007/s10533-023-01100-4, 2023.

Wei, J., Zhang, X., Xia, L., Yuan, W., Zhou, Z., and Brüggmann, N.: Role of chemical reactions in the nitrogenous trace gas emissions and nitrogen retention: A meta-analysis, Science of The Total Environment, 808, 152141, https://doi.org/10.1016/j.scitotenv.2021.152141, 2022.

Wilcock, R. J. and Sorrell, B. K.: Emissions of greenhouse gases CH_4 and N_2O from low-gradient streams in agriculturally developed catchments, Water, air, and soil pollution, 188, 155-170, https://doi.org/10.1007/s11270-007-9532-8, 2008.

Wimberly, M. C.: Geographic data science with R: Visualizing and analyzing environmental change, Chapman and Hall/CRC, https://doi.org/10.1201/9781003326199, 2023.

Wu, Z., Yu, D., Yu, Q., Liu, Q., Zhang, M., Dahlgren, R. A., Middelburg, J. J., Qu, L., Li, Q., and Guo, W.: Greenhouse gas emissions (CO_2–CH_4–N_2O) along a large reservoir-downstream river continuum: The role of seasonal hypoxia, Limnology and Oceanography, 69, 1015-1029, https://doi.org/10.1002/lno.12544, 2024.

Xu, X., Yang, Y., Zhou, Y., Ma, J., Li, J., Zhou, X., Zhao, X., Wu, F., and Song, K.: Global patterns and drivers of coupling between anammox and denitrification processes across inland aquatic ecosystems, Communications Earth & Environment, 6, 23, https://doi.org/10.1038/s43247-024-01980-w, 2025.

Yan, W., Li, J., Liang, J., Ye, C., and Yu, X.: Impact of dissolved oxygen levels on N_2O emissions and metabolically active bacterial community in biological nitrogen removal, Biochemical Engineering Journal, 206, 109295, https://doi.org/10.1016/j.bej.2024.109295, 2024.

Yang, P., Wang, D., Lai, D. Y., Zhang, Y., Guo, Q., Tan, L., Yang, H., Tong, C., and Li, X.: Spatial variations of N_2O fluxes across the water-air interface of mariculture ponds in a subtropical estuary in southeast China, Journal of Geophysical Research: Biogeosciences, 125, e2019JG005605, https://doi.org/10.1029/2019JG005605, 2020.

Yao, Y., Tian, H., Shi, H., Pan, S., Xu, R., Pan, N., and Canadell, J. G.: Increased global nitrous oxide emissions from streams and rivers in the Anthropocene, Nature Climate Change, 10, 138-142, https://doi.org/10.1038/s41558-019-0665-8, 2020.

Yoon, S., Heo, H., Han, H., Song, D.-U., Bakken, L. R., Frostegård, Å., and Yoon, S.: Suggested role of NosZ in preventing N_2O inhibition of dissimilatory nitrite reduction to ammonium, Mbio, 14, e01540-01523, https://doi.org/10.1128/mbio.01540-23, 2023.

Zhang, Q., Lin, L., Chen, Y., Wang, Y., Li, X., Li, L., Cao, W., and Zhang, Y.: Dual-edged effects and mechanisms of

https://doi.org/10.5194/essd-2026-109
Preprint. Discussion started: 13 May 2026

hydroxylamine in partial denitrification-anaerobic ammonium oxidation system, Environmental Research, 235, 116664, https://doi.org/10.1016/j.envres.2023.116664, 2023.

Zhang, L., Wang, X., Huang, L., Wang, C., Gao, Y., Peng, S., Canadell, J. G., and Piao, S.: Inventory of methane and nitrous oxide emissions from freshwater aquaculture in China, Communications Earth & Environment, 5, 531, https://doi.org/10.1038/s43247-024-01699-8, 2024.

Zhang, Z., Xia, X., Liu, S., Wang, J., Xu, W., McDowell, W. H., Tian, H., and Yang, Z.: Human-impacted lakes contribute over one-third of global lake greenhouse gas emissions, One Earth, https://doi.org/10.1016/j.oneear.2025.101568, 2026.

Zheng, Y., Wu, S., Xiao, S., Yu, K., Fang, X., Freeman, C., Liu, S., and Zou, J.: Global methane and nitrous oxide emissions from non-marine waters, https://doi.org/10.21203/rs.3.rs-744808/v1, 2021.

Zheng, Y., Wu, S., Xiao, S., Yu, K., Fang, X., Xia, L., Wang, J., Liu, S., Freeman, C., and Zou, J.: Global methane and nitrous oxide emissions from inland waters and estuaries, Global Change Biology, 28, 4713-4725, https://doi.org/10.1111/gcb.16233, 2022.

Zhu, J., Jia, Y., Yu, G., Wang, Q., He, N., Chen, Z., He, H., Zhu, X., Li, P., Zhang, F., Liu, X., Goulding, K., Fowler, D., and Vitousek, P.: Changing patterns of global nitrogen deposition driven by socio-economic development, Nature Communications, 16, 46, https://doi.org/10.1038/s41467-024-55606-y, 2025.